AMERICAN UNIVERSITY OF BEIRUT

# OPERATOR-BASED DYNAMIC BANDWIDTH MANAGEMENT FOR TELEOPERATION

by

HAYTHAM MOUNJI DBOUK

A thesis
submitted in partial fulfillment of the requirements
for the degree of Master of Engineering
to the Department of Electrical and Computer Engineering
of the Maroun Semaan Faculty of Engineering and Architecture
at the American University of Beirut

Beirut, Lebanon
January 2019

AMERICAN UNIVERSITY OF BEIRUT

# OPERATOR-BASED DYNAMIC BANDWIDTH MANAGEMENT FOR TELEOPERATION

by
HAYTHAM MOUNJI DBOUK

Approved by:

Prof. Imad Elhajj — Advisor
Dept. of Electrical and Computer Engineering, Professor

Prof. Naseem Daher — Member of Committee
Dept. of Electrical and Computer Engineering, Assistant Professor

Prof. Elie Shammas — Member of Committee
Dept. of Mechanical Engineering, Associate Professor

Date of thesis defense: January 28, 2019

# AMERICAN UNIVERSITY OF BEIRUT

# THESIS, DISSERTATION, PROJECT RELEASE FORM

Student Name:

| Dbouk | Haytham | Mounji |
|---|---|---|
| Last | First | Middle |

● Master's Thesis ○ Master's Project ○ Doctoral Dissertation

☐ I authorize the American University of Beirut to: (a) reproduce hard or electronic copies of my thesis, dissertation, or project; (b) include such copies in the archives and digital repositories of the University; and (c) make freely available such copies to third parties for research or educational purposes.

☑ I authorize the American University of Beirut, to: (a) reproduce hard or electronic copies of it; (b) include such copies in the archives and digital repositories of the University; and (c) make freely available such copies to third parties for research or educational purposes after:

**One ---- year from the date of submission of my thesis, dissertation, or project.**

**Two ---- years from the date of submission of my thesis, dissertation, or project.**

**Three ---- years from the date of submission of my thesis, dissertation, or project.**

Signature

6/2/2019

Date

# ACKNOWLEDGMENTS

I would like to first start by thanking Allah for his mercy and blessings that without them I would not have completed this thesis. Second, I would like to thank my family who have been my source of strength and motivation to reach my goals for this life and the one after. I would like to also thank my father for being a real influencer all over this journey, and my mother for being the blessing in my life.

I would like to thank my advisor, Prof. Imad H. Elhajj, whose guidance, understanding, support, and patience enhanced my graduate experience.

Also I would like to thank my committee members Prof. Naseem Daher and Prof. Elie Shammas for their support all over this journey.

Finally, I would like to acknowledge the Lebanese National Counsel for Scientific Research and the AUB University Research Board for funding this research.

# AN ABSTRACT OF THE THESIS OF

Haytham Mounji Dbouk for Master of Engineering
Major: Control and Robotics

Title: Operator-Based Dynamic Bandwidth Management for Teleoperation

Teleoperation has become a common feature in most systems and is now integrated into the control of collaborative robots' swarms from a remote area. This thesis presents the design and development of a real time operator-based dynamic bandwidth management scheme for teleoperation of swarms of collaborative robots. This method is effective in complex teleoperation tasks that require the collaboration of several robots instead of a single robot. This thesis integrates personalization with bandwidth allocation through a novel two-level controller which dynamically updates the distribution of the available bandwidth among the robots to user (R2U), robot to robot (R2R) and user to robots (U2R) communication channels. This is accomplished through an optimization method using real-time observations. These observations reflect 1) changes in the personalizing factor (PF) through the changes in the level of disturbance encountered by the operator, 2) changes in quality of collaboration (QoC) of the executed task, along with 3) the occurrence of Interesting events (IEs) in the swarm's environment. This optimization ensures the effective accomplishment of the collaborative task with lower bandwidth consumption and better performance. The designed closed-loop two-level controller includes: Level 1, an event-based fuzzy logic controller triggered by the performance measures sent by the robot and results in the appropriate set of constraints; Level 2, a time-based triggered Lagrange optimization algorithm which determines the updated set of R2U, R2R and U2R communication rates. The designed operator-based dynamic bandwidth management algorithm is compared against the dynamic bandwidth management algorithm developed by Mansour et al. MATLAB simulations and experiments using humanoid robots were conducted. The comparison carried out in both validations demonstrates the superiority of the operator-based dynamic bandwidth management algorithm in terms of task and network performance. The performed simulations and experiments show that the designed two-level controller out-performs the dynamic bandwidth management algorithm in terms of the task duration, the covered distance and the encountered errors as well as the required effort.

# CONTENTS

ACKNOWLEDGMENTS ..... v

CONTENTS ..... vii

ILLUSTRATIONS ..... x

TABLES ..... xi

Chapter

1. INTRODUCTION ..... 1

2. LITERATURE REVIEW ..... 5

2.1 Preamble ..... 5

2.2 Collaborative Robotics ..... 5

2.3 Teleoperation ..... 7

2.4 Bandwidth Management ..... 9

2.5 Human Machine Interface ..... 11

3. Problem Formulation ..... 14

3.1 Preamble ..... 14

3.2 General Formulation ..... 15

3.2.1 Operator-Aware Bandwidth Management Algorithm ..... 16

3.2.2 Two-level controller General Design ..... 17

3.3 Application Description ..... 23

3.4 Two-level controller solution of the optimization problem ..... 29

3.4.1 M matrix Division into Clusters/Groups ..... 29

3.4.2 Qualitative Rules Generation ..... 30

3.4.3 Fuzzy Logic Controller Design ..... 31

3.4.4 Level 2 Constraints Generation ..... 31

3.4.5 Lagrange Optimization Design ..... 33

3.4.6 Bandwidth Rates Determination ..... 35

4. SIMULATION & RESULTS ..... 37

4.1 Preamble ..... 37

4.2 MATLAB validation simulation ..... 37

4.2.1 MATLAB Disturbance Presence Results ..... 39

4.2.2 MATLAB Disturbance Absence Results ..... 40

4.3 WEBOTS scaling simulation ..... 41

4.3.1 WEBOTS Disturbance Presence Results ..... 44

4.3.2 WEBOTS Disturbance Absence Results ..... 44

5. EXPERIMENTAL SETUP AND RESULTS ..... 46

5.1 Preamble ..... 46

5.2 System Description ..... 46

5.2.1 NAO Humanoid Robots ..... 48

5.2.2 Sensory Readings ..... 49

5.3 Experimental Setup ..... 50

5.4 Testing Scenarios ..... 51

5.5 Experimental Execution & Results ..... 55

5.5.1 Experimental Disturbance Presence Results ..... 55

5.5.2 Experimental Disturbance Absence Results ..... 56

5.5.3 Experimental Results Summary of two-level controller ..... 57

5.5.4 NASA Disturbance Presence Results ..... 58

5.5.5 NASA Disturbance Absence Results ..... 59

6. CONCLUSION AND FUTURE WORK ..... 60

REFERENCES ..... 64

APPENDIX ..... 69

# ILLUSTRATIONS

Figure Page

Figure 1 Teleoperation session ..... 2

Figure 2 Fuzzy controller composition ..... 20

Figure 3 Closed loop 2 levels control scheme ..... 22

Figure 4 Two robots in a formation that requires a fixed distance (D=60cm) ... 24

Figure 5 Operator-Based Dynamic Bandwidth Management scheme ..... 28

Figure 6 M matrix grouping ..... 29

Figure 7 Sample of the conducted tele-operation task ..... 38

Figure 12 NAO Humanoid Robot ..... 48

Figure 14 Communication scheme ..... 50

Figure 15 Experimental Setup ..... 51

Figure 16 Humanoid Robots' path and alignment ..... 52

# TABLES

Table Page

Table 1 MATLAB simulation disturbance presence scenario results ..... 39

Table 2 MATLAB simulation disturbance absence scenario results..... 40

Table 3 WEBOTS simulation disturbance presence scenario results..... 44

Table 4 WEBOTS simulation disturbance absence scenario results ..... 45

Table 5 Experimental disturbance presence scenario results..... 55

Table 6 Experimental disturbance absence scenario results..... 56

Table 7 Experimental Results for the designed two-level controller..... 57

Table 8 NASA form disturbance presence scenario results ..... 58

Table 9 NASA form disturbance absence scenario results..... 59

# CHAPTER 1

# INTRODUCTION

Teleoperation has various applications including but not limited to tele-manipulation in environments which are inaccessible or remote such as space and deep sea exploration [4], [6] nano and micro teleoperation [5], tele-surgery [8], exploration of disaster zone, construction in space, hazardous materials' handling, and rescue [37]. Furthermore, teleoperation is an essential approach to control mobile robot swarms. Yet, guaranteeing a minimum control quality necessitates the availability of specific network resources, which generate an optimal execution of the conducted task. Song et al. [38] and Palafox et al. [39] elaborated on the two major constraints on the "Robot" to "User" (R2U), "User" to "Robot" (U2R), and "Robot" to "Robot" (R2R) communication channels. This work stresses on the transmission quality of the captured images, the generated commands from the operator to control the swarms of robots (U2R) and the sensed data by the collaborative robots to be sent to the operator to adapt accordingly (R2U). Moreover, Palafox et al. [39] concentrate on the dilemma of transmission delays.

A network-based teleoperation scheme includes distant interactions between remote robots' swarms and human operator(s) [11]. Teleoperated schemes have been under continuous research specially the ones operating in the presence of different network constraints such as packet loss, limited bandwidth, demanding CPU processing time and various time delays. Constraints such as CPU processing and limited bandwidth availability cause the degradation of the Quality of Service (QoS) to the extent that can severely affect the collaborative task performance [20]. Maintaining a

level of task performance that guarantees an appropriate QoS within distributed multimedia systems is done through implementing several bandwidth management algorithms [11]. Yet, the issue of bandwidth management based on the robots' quality of collaboration along with sensory feedback, was has not been investigated. For example, collaborating robot swarms' teleoperation within a remote environment requires all the involved agents to exchange large amount of information. Operator(s) transmit real-time commands to the collaborating robot swarms, and accordingly receive instantaneous haptic and visual feedback expressing operator(s) performance within the task execution along with the corresponding environment trait. In addition, throughout the collaborative task execution the involved robots' swarms continuously exchange mutual data among each other to preserve appropriate levels of cooperation (Figure 1).

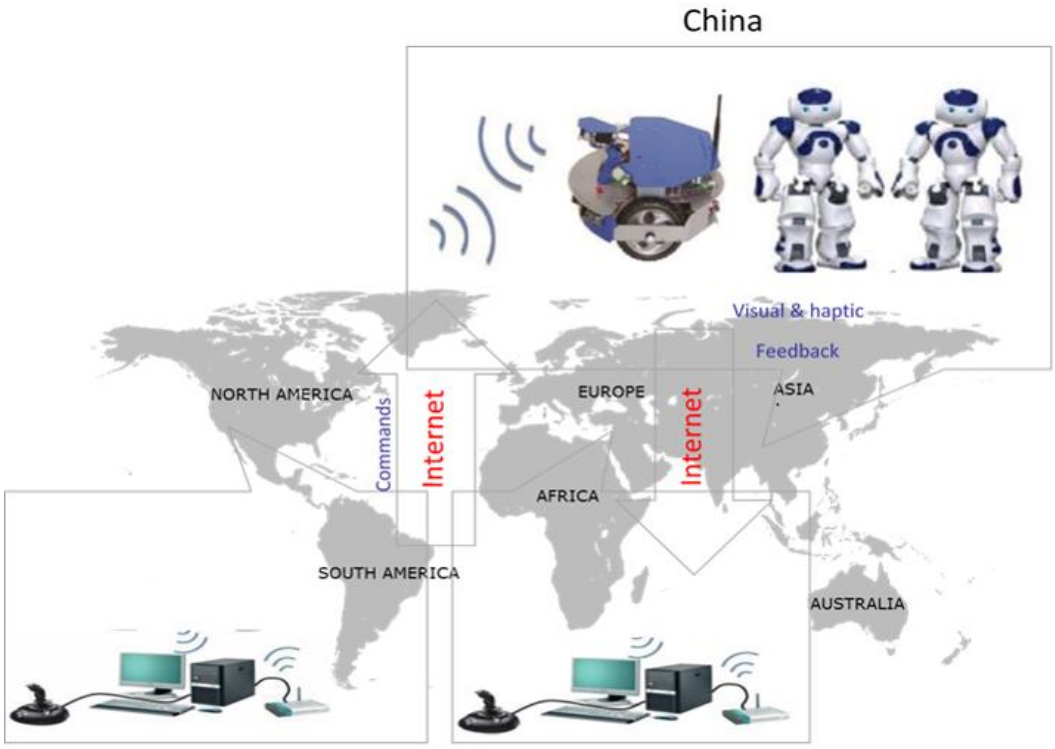


*Figure 1 Teleoperation session*

This work represents real-time optimized operator-based dynamic bandwidth management for teleoperation of collaborative mobile robots. The proposed operator-based dynamic bandwidth management algorithm integrates the PF into the bandwidth scheme through a two-level controller which dynamically updates the corresponding real-time distribution of the available bandwidth among the R2U, R2R and U2R communication channels in a way

to optimize performance, upon receiving a new set of real-time observations. These observations reflect 1) changes in the personalizing factor (PF) through the changes in the level of disturbance encountered by the operator, 2) changes in quality of collaboration (QoC) of the executed task, along with 3) the occurrence of interesting events (IEs) in the swarm's environment. The operator-based dynamic bandwidth management accounts for any deficiency in the swarms' collaborative task to ensure the effective accomplishment of the collaborative task with lower bandwidth consumption and better performance. For instance, in a mission requiring that the swarm preserves a specific formation (relative orientation and position), the errors in orientation ($\Delta\alpha$) and position ($\Delta y$ and $\Delta x$) between robot pairs are explicit illustrations of objective quantities showing the change in the collaborative task quality.

The most relevant work in the domains of collaborative robots, teleoperation, bandwidth management and human machine interface is presented in Chapter 2. Chapter 3 presents the detailed problem formulation followed by the MATLAB implementation of the designed two-level controller. The designed two-level controller is then implemented on a specific application which requires the navigation of two humanoid robots through a predefined track while avoiding the track obstacles. Chapter 4 represents a detailed MATLAB simulation implementing the two-level controller and

the dynamic bandwidth management scheme designed by Mansour [1, 2] and compares both algorithms in the presence and absence of disturbance in a way to integrate the PF as a major factor for the bandwidth distribution scheme. This simulation is followed then by another simulation using WEBOTS to scale up the task conditions along with the corresponding number of robots, this simulation is used to show the efficiency and the applicability of the implemented two-level controller in more complicated tasks. Furthermore, Chapter 5 presents the experimental application implementing the designed two-level controller. The proposed algorithm is evaluated against the dynamic bandwidth management algorithm presented by Mansour [1, 2]. Finally, conclusions of the proposed algorithm are illustrated, and future research suggestions are indicated in Chapter 6.

# CHAPTER 2

# LITERATURE REVIEW

## 2.1 Preamble

Chapter 2 presents a survey of the recent work done on bandwidth management in the domain of teleoperation of collaborative robots. The first section presents an overview of the various collaborative robots then section 2 presents the most important methods of teleoperation integrated to drive and operate robot swarms. Section 3 presents the various bandwidth management schemes applied in the teleoperation of robots' swarms. Finally, section 4 presents an overview of the work done in the domain of human machine interface to serve the task of teleoperation and allow for the adaptability of the teleoperation management scheme along with the changes of the task conditions and its reflection on the operator.

## 2.2 Collaborative Robotics

Robot swarms are extensively engaged in composite tasks that cannot be achieved by a sole robot or in tasks that are accomplished better through robots' collaboration. The conducted review demonstrates various tasks executed by collaborating robots' swarms: formation localization [14], tracking of target [15], localization and mapping [16], estimation of state [40], exploration [41], pushing of an object [42], and radar jamming [43]. For example, Sugiyama et al. [15] investigates multi-robot structures and their wireless networks' QoS. A Disaster area is scanned by a swarm of mobile robots watching for potential survivors or victims. Upon detecting a

victim within this rescue operation, the information is sent by the corresponding robot to the base-station. Furthermore, Bhuvanagiri et al. [16] presents a new method for the problem of localizing a swarm of mobile robots'. The robots are allowed to have several hypotheses of their relative position through equipping them with the ability to detect each other. This challenge is resolved over two consecutive steps: first active localization is figured followed by coordinated localization. The offered scheme presents a combined probabilistic context which accounts for both the local map structure measurements along with the measurements' role between robots upon determining the finest goal locations. The technique obtains utility in various scenarios for multi-robot, in which robots have various hypotheses and accordingly necessitate other robots' assistance to resolve vagueness in addition to improve their state estimates accuracy. Moreover, state estimation integrates the effort of collaborative mobile robots [40]. Unmanned Ground Vehicles (UGVs) as well as Unmanned Arial Vehicles (UAVs) collaborate so as to trail and approximate the corresponding UGV states. The corresponding UAV's avionics and sensors are combined together, combining the equations of the UGV kinematics algorithms, and the algorithms implemented for geo-positioning of the UAV to formulate a robust UGV state estimation. Both simulations and experiments were performed to find the geo-positioning accuracy by means of the aircraft structure. Both simulation and experimental results demonstrate similar outcomes which validate the implemented UGV's state estimation algorithm. Jiang et al. [41] shed the light on the challenge of multiple autonomous underwater vehicle structure coordinated control within tasks in the real-world including oceanographic sampling and environmental exploration. Hence, this work realizes underwater vehicles' fully distributed control and vehicles' timely reaction is ensured through integrating

behavior-based control approach in dynamic and complex environment. Hu et al. [42] targets box-pushing tasks in underwater environment through cascading three autonomous robotic fish system. The robotic fish is enabled to approximate the pose of the object in the swimming tank using the monocular camera onboard. Bearing in mind the restricted capabilities of a sole robotic fish and the complication of the underwater environment, the task is addressed by splitting it into three subtasks and allocating them to adequate robotic fish. Thus, robotic fish manage over explicit communications and allocate the subtasks through a market-based dynamic task distribution algorithm. Furthermore, environment exploration is an application which employs collaborative mobile robots. Radar jamming is one more application which employs collaborative robots [43]. A group of Unmanned Arial Vehicles (UAVs) collaborate to mislead a ground radar network to see a phantom path in its radar space. This work develops a radar deception challenge real-time motion planning scheme to design singular trajectories' reference which can supremely end up with a zero error in formation within the stage of tracking control; however continuously monitoring the dynamic feasibility concern which is ignored by most methods of multi-agent systems' formation control. Yet, a remarkable glitch in this method is that the synchronized communication is non-realistic because of the unavoidable time-delays.

## 2.3 **Teleoperation**

Teleoperation is the process during which a human operator, interacts with a master device to remotely control the motion of a slave device [3, 31]. Teleoperation plays a major role in various environments in which the direct physical interaction between the human operator and the teleoperated object is not feasible [3]. This case is

present in a variety of applications such as tele-surgery [7, 8, 9, 12, 13, 34], nano-teleoperation [6, 23], iconic gestures [24] etc. These environments are either hazardous, highly uncertain [33], geometrically or physically constrained, or distant task environments [4, 5].

A network-based teleoperation system includes distant interactions between human operator(s) and remote robotic systems [10, 11, 27], in which different network constraints are present such as bandwidth, packet loss, and time delay [32]. Furthermore, swarms of robots are commonly employed in complex tasks which can't be achieved by a single robot or in certain tasks which are preferably performed by collaborated robots such as localization in formation [14], target tracking [15], mapping and localization [16, 18], object pushing [17], etc. Li, Tadano, and Kawashima [9] state that the different components of the teleoperation system: operator, communication channel, remote environment, and sensors, introduce a set of uncertainties in the system [9]. The system should be stable with respect to this set of uncertainties. Thus specific network constraints should be fulfilled upon the teleoperation of mobile robot swarms to assure minimum quality of control (QoC) resulting in effective task accomplishment [19, 28]. Constraints such as CPU processing and bandwidth cause degradation of the Quality of Service (QoS) of teleoperated systems to a level that severely affects the performance [20, 21]. Hence, several bandwidth management algorithms have been designed and implemented for scattered multimedia systems so as to preserve a performance which secure an acceptable QoS [10, 22, 25, 26]. The proposed algorithm builds on the real-time dynamic optimized bandwidth management algorithm for collaborative teleoperated robots presented by Mansour et al. [1], which handles the problem of managing bandwidth based on sensory feedback and the quality of

collaboration among robots. The optimization algorithm presented in [1, 2] accounts for Interesting Events (IEs) and the change in the Quality of Control (QoC) between the teleoperated swarm of robots to adapt the bandwidth allocation between the acting agent, where necessary, in a certain environment. The main contribution of this work is that it cascades the Personalizing Factor (PF) as an additional optimization factor to the bandwidth management algorithm [1, 2] to present a user dependent real-time dynamic optimized bandwidth management algorithm for collaborative teleoperated robots.

## 2.4 **Bandwidth Management**

Different approaches of bandwidth management protocols are adopted to resolve the network resources sharing problem in robotic systems. These protocols in networked control systems fall into two main groups: static [29] and dynamic [25, 30] bandwidth distribution. Static protocols cannot adjust to changes in the system state (nearby environment, collaboration quality, service quality etc.). On the other hand, dynamic bandwidth management methods enhance the performance of the teleoperated system with the cost of higher complexity. In [14] Mourikis et al. address the problem of resource allocation in formations of mobile robots localizing as a group. The goal is to determine the frequency at which each individual sensor is to be used in order to achieve the highest possible localization accuracy. Moreover, the set of frequencies declared is obtained by solving an optimization problem that maximizes the accuracy matrix expressed in terms of sensor frequencies. Yet, the problem is solved offline and the algorithm does not account for any dynamic events that might occur. Sugiyama et al. [15] propose a bandwidth reservation algorithm for multi-robot systems for a target tracking mission. The interesting information, corresponding to a survivor's detection,

is sent to the base station with wideband signals such as dynamic picture images. The final call is left for the operators to decide whether the received images indicate a real victim, by allowing/preventing the corresponding robot to reserve the bandwidth affecting the flow of various signals from other robots to the base station. In this approach, the operator's intervention is crucial in allocating bandwidth and thus the allocation process is not fully automated. Xi et al. [11] developed a bandwidth allocation mechanism based on online measured task dexterity index of dynamic tasks so that operators can control remote manipulators efficiently and smoothly even under poor network quality. However, the executed task is simple and does not require the collaboration of multiple robots to be performed. Thus, the quality of collaboration factor is not considered in the bandwidth allocation. Finally, in [17], a bandwidth management algorithm is introduced and the rate of feedback is regulated based on the amount of activities occurring in the environment. The work shows that during complex tasks, the operator's performance is affected by the rate of feedback of information. It is also confirmed that a higher sampling rate is required to maintain the same level of performance obtained when the environment is less dynamic. Yet, the implemented algorithm does not impose any constraint on the total bandwidth of the system. In addition, the notion of monitoring changes in QoC to allocate bandwidth is not mentioned since the task execution only requires the use of a single robot. To the best of the author's knowledge, there was limited research addressing bandwidth management for the specific application of collaborative robots' teleoperation. In 2015, Ricardo and Guilherme designed a Dynamic Bandwidth Management Library to control the frequency of individual sensors present in a robotic environment performing a certain task [35]. This work is pursuing a universal Dynamic Bandwidth Management Library

designed to be used on a system with a variable number of heterogeneous robots performing any collaborative task that requires communication transactions such as the exchange of sensor data between involved agents.

## 2.5 Human Machine Interface

Work in human machine interface field is divided into two main approaches which are user-dependent approach and user-independent approach. The user-dependent approach has three main aspects: learning schemes, performance-based schemes, and enhancements-based schemes, while the user-independent approach has two main aspects: learning schemes along with performance based statistical normalizing schemes.

T. Langner et al. [44] presents a user-dependent performance-based system which constantly monitors the driver's level of attention in traffic, helping the user to focus on crucial traffic situations. The vehicle is instrumented and can identify the state of traffic-lights, as well as obstacles on the road. If the driver is inattentive and fails to recognize a threat, the assistance system produces a warning. The proposed system consists of three components: computer vision detection of traffic-lights and other traffic participants, an eye tracking device used also for head localization, and finally, a human machine interface consisting of a head-up display and an acoustic module used to provide warnings to the driver. L. Roche et al. [23] represents a user-based learning approach experimental evaluation of physical human-human interaction in lightweight condition using a one degree of freedom robotized setup. It explores possible origins of Physical Human-Human communication, more precisely, the hypothesis of a time-based communication. To explore if the communication is correlated to time a statistical state

machine model based on physical Human-Human interaction is proposed. Moreover, P. Berthet- Rayne et al. [12] proposes a novel enhancement-based three-state Human-Robot cooperative control framework for bimanual surgical tasks: integrating human-robot cooperative control combining feature techniques such as active constraints, machine learning and automated movements into a framework which can be generalized to a wide range of surgical tasks. Thus, the proposed algorithm allows for seamless and automatic transitions between three different modes, depending on the current step of the surgical procedure: automated, manual with haptic guidance and finally fully manual.

Furthermore, Anbin Xiong et al. [45] presents a user-independent learning-based sEMG recognition method which is applicable to multi-users. First, single channel sEMG is decomposed into 30 MUAPTs, which includes four steps: two-order differential filter, threshold calculation, spike detection and hierarchical clustering. Secondly, the MUAPTs are updated with the templates orthogonalization; and Deep Boltzman Machine is employed to classify the MUAPTs into five classes corresponding to the predefined five gestures. K. Nakadai et al. [46] represents a performance-based Robot-Audition based Car Human Machine Interface (RA-CHMI) capable of dealing with the difficulty of distinguishing voice commands due to the many sources of noise in a car. Therefore, a microphone array processing is developed to replace the conventional single microphone, to overcome the noise problem. Moreover, Robot Audition techniques, including sound source localization, Voice Activity Detection (VAD), sound source separation, and barge-in-able processing, were introduced by considering the characteristics of RA-CHMI. Automatic Speech Recognition (ASR), based on a Deep Neural Network (DNN).

Based on the above literature, the presented method concentrates on managing the distribution of the total available bandwidth over the various R2R, U2R, and R2U communication channels for the swarm of teleoperated collaborating robots in order to assure optimized task performance while encountering network bandwidth bottlenecks. These bottlenecks may be due to limitations in the network at the robots or operator end. **The proposed bandwidth management algorithm is instituted on changes in PF, on variations in swarm of robots' QoC and on IEs occurring in the environment of the robot swarms.**

# CHAPTER 3

# PROBLEM FORMULATION

## 3.1 Preamble

The focus of the work presented is to optimize the real-time dynamic management of the ‘User’ to ‘Robot’ and ‘Robot’ to ‘User’ (U2R/R2U) and ‘Robot’ to ‘Robot’ (R2R) communication channels presented by Mansour et al. [1, 2], where actuation commands, system state and sensory data including video frames are exchanged. This is done through an operator-based adaptive bandwidth management algorithm for collaborative tele-operating robots. The presented algorithm monitors the occurring events in the robots’ environment and the change in quality of collaboration among robots, in addition to accounting for the personalizing factor (accounts for disturbance presence/absence). Consequently, a novel two-level controller is dynamically updating the bandwidth management scheme, upon recording a new set of observations. These observations reflect 1) changes in the *PF* through the changes in the level of disturbance encountered by the operator, 2) changes in *QoC* of the executed task, along with 3) the occurrence of *IEs* in swarm's environment. Hence, this ensures effective accomplishment of the collaborative task with better performance and lower bandwidth consumption.

General formulation of the problem is first presented; this can be applied with a variable number of collaborating robot swarms. The presented algorithm can also be applied to a variety of collaborative tasks performed by robot swarms taking into consideration that all the communication rates are precisely declared. Then this general

problem formulation is applied into a specific application where the collaborative task is to navigate two humanoid robots through a delimited path to reach a predetermined destination while avoiding obstacles and preserving a formation. Chapter 3 is then concluded by presenting the novel two-level controller design and specifications along with its MATLAB implementation to this optimization problem.

## 3.2 General Formulation

The objective is to establish Operator-Based Dynamic Bandwidth Management for Teleoperation, considering that the operator needs to be updated more frequently in the presence of disturbance. Updating the Bandwidth Management for Tele-operation according to the operator needs retaining the same level of performance all over the tele-operation task. In other words, the rates of information exchanged between the operator(s) and robots are updated based on changes in task conditions that may affect the performance severely. Similarly, the increase in R2R communication compensates for any decay in the performance of the collaborative task of the robotic swarm. Hence, if the environment is less dynamic and the robots are collaborating well, the corresponding communication rates will decrease. On the other hand, if the environment is more dynamic and the robots are collaborating poorly, the corresponding communication rates will increase. Let the collaborative task be executed by n robots and let $X_i$, where $i \in \{1, 2, \ldots, r\}$, be the communication rates to be optimized. Then, we define X as an r-dimensional vector of communication rates.

Moreover, P is defined as an m-dimensional matrix of the robots' observations, which accounts for various task conditions which can include but are not limited to:

1) The interesting events (IE) in the environment

2) The quality of collaboration (QoC) of the robots and

3) The personalizing factor (PF), Where

$$P = \begin{bmatrix} P1 \\ P2 \\ . \\ . \\ . \\ Pm \end{bmatrix} = \begin{bmatrix} IE \\ QoC \\ PF \end{bmatrix} \quad (1) \qquad X = \begin{bmatrix} x1 \\ x2 \\ . \\ . \\ . \\ xr \end{bmatrix} = M\,P \quad (2)$$

Where each element of P is normalized with respect to the maximum value of the corresponding observation in a way to solve this optimization problem. Moreover, knowing that M is a rxm matrix representing the weights for the corresponding performance measures (P values); thus it should dynamically adapt to the IEs, QoC and the PF to increase the efficiency and optimality of this operator-based bandwidth management scheme. Hence the corresponding M matrix has to change values accordingly to adapt with the various changes within the tele-operation task, so that the bandwidth management is optimized in real-time considering the corresponding task conditions at each point in time.

### 3.2.1 *Operator-Aware Bandwidth Management Algorithm*

Considering that operator-based bandwidth management scheme is a human related control scheme with a variety of uncertainties, it is said to be: (1) non-linear, (2) ill-defined and (3) complex. A closed loop two-level controller is implemented in a way

to mimic the human mind set and cope with the need of adaptively updating the bandwidth distribution to optimize the user experience and thus the task performance. Accordingly, the designed controller is composed of two levels, level 1 is a fuzzy logic event-based controller triggered by the performance measures sent from the robot and results in the appropriate set of constraints for the M matrix accordingly. Moreover, the appropriate set of constraints determined by the level 1 controller are fed to the level 2 time-based optimization algorithm to guide the optimization scheme, to determine the optimal Lagrange based solution for the current state. Thus, the Fuzzy Logic controller is designed and implemented parallel to the optimization algorithm as a second-degree of control triggered by the corresponding feedback values from the tele-operated robots. The designed two-level controller includes a fuzzy logic controller. Consequently, the closed-loop fuzzy logic controller is used to accomplish the task of transforming the intuition of dynamically changing the M matrix values into a set of organized and well-defined inference rules which are fed as constraints to the Lagrange-based optimization tool. The optimization tool will assure that the M matrix will dynamically adapt with the IEs, QoC and PF to ensure the optimum distribution of the available bandwidth in real-time.

### 3.2.2 *Two-level controller General Design*

Considering the two-level hybrid control theory, a divide and conquer approach will be followed to fulfil these requirements. The steps for the two-level hybrid control theory are:

#### 3.2.2.1 M Matrix Division into Clusters/Groups

Divide the M matrix into clusters/groups of similar rows **[rows that depend on the same performance factors]**, this step reflects the intuition specific for each application case.

#### 3.2.2.2 Qualitative Rules Generation

Generate the corresponding qualitative rules; consider available heuristics where reverse engineering is implemented to determine the set of performance [P] measures that each group depends on. These rules are used then as the input to the level 1 fuzzy controller.

#### 3.2.2.3 Fuzzy Logic Controller Design

Design the appropriate fuzzy logic controller and accordingly the input-output relationship which takes the intuition qualitative rules as inputs and gives the M matrix weights as output **[Level 1 output, which will be fed then to the optimization algorithm].**

Fuzzy control is the theory of computing with words, it is the theory which uses qualitative factors and measures to control a certain process usually due to the unavailability of an accurate mathematical model of the process. Thus, fuzzy logic depends on the concept of classifying the process inputs into distinguishable sets and consider the membership (belonging factor which is a given value between 0 and 1) to these various sets as a key factor for the decision on the appropriate output corresponding to the given input. The degree of membership – 0 = doesn't belongs, 1 = belong, and any other value between 0

and 1 corresponds to a partial membership- represents the degree of compatibility with the property defining the corresponding fuzzy set.

Moreover, the designed membership functions need to overlap and cover the entire range of each input of the controller (the performance measures feedback/P vector in our case), allowing for the decision making at the level of the controller output under the present of uncertainties and interesting events taking place in the dynamic process environment. This is done through developing the appropriate fuzzy relations between the fuzzy sets, in a way to mimic the human intelligence and prevent the undesirable consequences. This has two main ways:

- Trial and error: it is the black box analogy; due to the absence of sufficient information we consider educated guesses for the fuzzy relations, yet this is difficult and time consuming.
- Systematic procedure: it is the grey box analogy; benefiting from the presence of available input-output relationship and considering any possible learning algorithm, the fuzzy relations are derived.

Therefore in our application where we have a well-defined optimization problem along with a specified mathematical formulation of the bandwidth distribution scheme, we will consider the systematic procedure as a complement for the designed optimization algorithm. For this we need to consider the fuzzy logic architecture shown in figure 2 in the formulation of our fuzzy logic scheme.

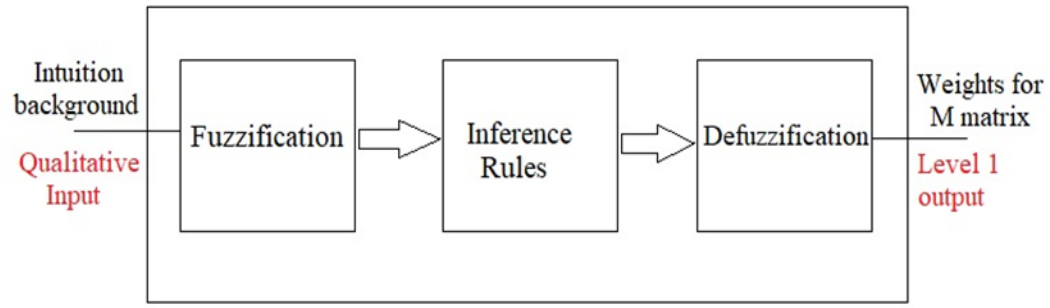


*Figure 2 Fuzzy controller composition*

In our application we have 2 design approaches which can be used to implement the necessary fuzzy logic bandwidth management algorithm for the conducted Teleoperation task.

**Approach 1:** Implement full fuzzy logic algorithm which will handle alone the bandwidth management, this is done through transforming the whole input-output relationship of the conducted process into a set of N Extended Inference rules [System transfer function is assumed unknown].

**Approach 2:** Implement a hybrid Event/time triggered controller, which consists of a two-level controller. The fuzzy logic tool is used here as a guidance for the mathematical optimization problem/solution, so that it will give the weights [L, M, H] for each group of rows according to a group of Extended Inference rules.

Furthermore, considering the fact that we have a well-defined optimization problem along with a specified mathematical formulation of the bandwidth distribution scheme, we will consider the second approach shown in figure 3. Consequently, the fuzzy Logic controller is designed and implemented parallel

to the optimization algorithm as a second degree of control, this will translate into a group of constraints and conditions all over the optimization solution [fuzzy decisional algorithm]. So we have two-level control 1) The implemented fuzzy logic, weight control and 2) Lagrange based optimization scheme for the M matrix.

#### 3.2.2.4 Level 2 Constraints Generation

The designed fuzzy logic controller algorithm is composed of the implemented fuzzy relations; these relations link the qualitative measures/rules real-time performance measures inputs and the resulting weights for the M matrix **[Level 1 output, which will be fed to the optimization level 2 control].** Moreover, as discussed and decided before, these fuzzy relations are set in a systematic manner considering the environment where the teleoperation task is taking place, the occurring interesting events, and the respected constraints throughout the design process.

Develop the obtained weights for the M matrix **[Level 1 output]** as constraints and conditions which will be fed to the optimization algorithm that will adapt to this set of constraints. Figure 3 presents the overview of the implemented two-level controller; the two-level controller is responsible for determining the appropriate M matrix in real-time:

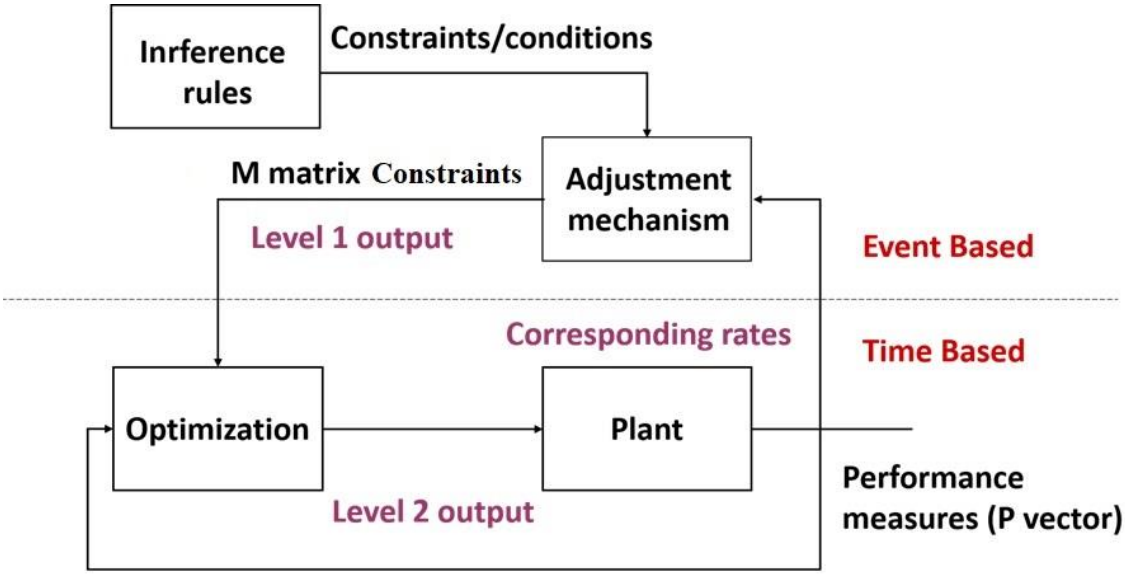


*Figure 3 Closed loop 2 levels control scheme*

Challenging problems in the design of fuzzy inference systems:

Setting of the input and output membership functions **[Range and Shape]**

Setting of the inference rules; that is the fuzzy relation by which input combinations correspond to which output.

Selection of the fuzzy logic operations which will translate the fuzzy logic operations **[And, Or, Then]**

Selection of the appropriate fuzzy set **[Defuzzification method; learning due to the lack of a learning function]**

Note: Consider each of the different row groups to have different membership function over all columns inputs; knowing that each group has different characteristics and dependence on the columns inputs.

#### 3.2.2.5 Lagrange Optimization Design

Design the appropriate Lagrange based optimization controller and feed it the previously derived constraints considering the cost function we are working on.

We define for the bandwidth optimization the cost function:

$$\sum_{i=1}^{r} \mathbf{w_i x_i} - \mathbf{B_{max}} \leq \mathbf{0} \qquad (3)$$

Knowing that the sum of inputs of each row of the M matrix is 1. The implemented optimization scheme will consider the bandwidth management cost function and the real-time obtained constraints set from the **fuzzy level 1 controller** to obtain the appropriate values for the M matrix entries in a manner to adapt with the system status. Then, we use these entries to determine the real-time bandwidth rates **[first output of the level 2 controller]**.

#### 3.2.2.6 Bandwidth Rates Determination

Develop the corresponding real-time output of the optimization algorithm **[Level 2 output]** as shown in (2).

## 3.3 Application Description

This section illustrates the implementation of the designed two-level controller into a specific application in which an operator is asked to navigate two humanoid robots through a delimited path to reach a predetermined destination while avoiding obstacles and preserving a specific formation. The operator recognizes the environment through the cameras of the robots; thus the robots' feedback includes both haptic and

visual information reflecting the environment current status. The task to be accomplished by the 2 collaborating robots is to sustain a specific formation through a delimited path to reach a predetermined destination while avoiding obstacles. Moreover, the specific formation is shown in figure 4 while the horizontal alignment is nearly zero, and keeping a vertical distance of 60cm separating the two robots.

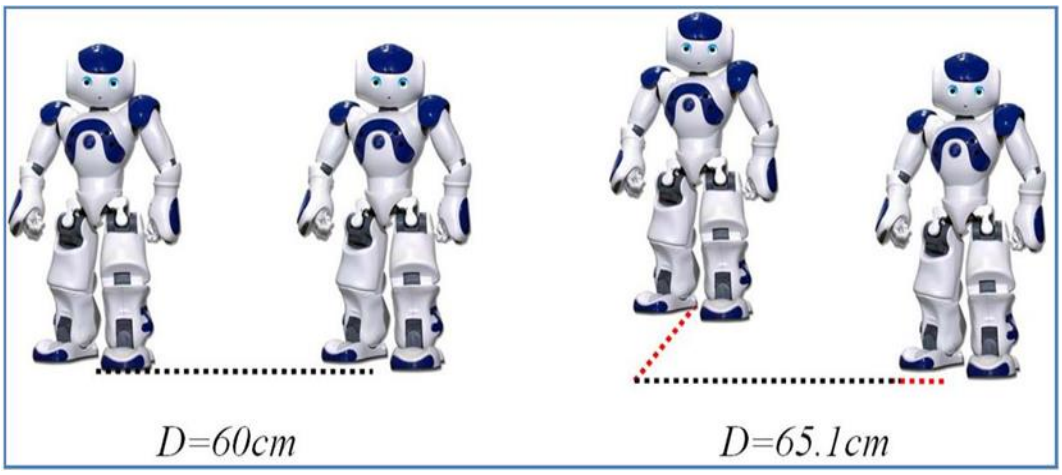


*Figure 4 Two robots in a formation that requires a fixed distance (D=60cm)*

*a) Without Error* *b) With Vertical & Horizontal Errors*

This formation represents a plain concept upon which any interaction-based task can be built rather than just a specific task performing interaction by itself. Thus, the operator is asked to navigate the two humanoid robots through a delimited path to reach a predetermined destination from an exact stating point while avoiding obstacles and preserving a specific formation. Moreover, the detection of the obstacles in the navigation path is done through three ultrasonic sensors fixed on the right, left and front side of each robot. An integer value is returned by each sensor, representing the distance to the nearest obstacle distinguished. Besides, the visual feedback of the space in front of the formation is provided through the camera fixed on top of each robot.

To manage the available bandwidth considering the personalizing factor, the level of disturbance encountered by the operator during the teleoperation task is integrated into the bandwidth management scheme. The concept is that the visual and haptic feedback rates delivered to the operator will increase with the presence of disturbance in order to maintain a high performance, similarly the visual and haptic feedback rates will decrease with the absence of disturbance. Moreover, the bandwidth management scheme accounts for the IEs (changes in the task conditions) through monitoring the speed of the swarm and the corresponding distance between each robot and the obstacles. Thus, regardless of the absence of obstacles in the swarm path, the user will require higher visual and haptic feedback rates in order to preserve high performance upon driving at a higher speed. Accordingly, the swarm's speed is one of the dynamic events considered upon the rates allocation. Furthermore, QoC factors are indications of the robots' collaboration efficiency to fulfill the collaborative task. Besides, $\Delta x$ and $\Delta y$ the position errors between the robot pair are monitored considering that they reflect the change in the quality of collaboration of the specified task.

Hence, based on real-time observations related to changes in the level of disturbance, occurrences of environment IEs, and changes in QoC between robots during the task performance, the R2U haptic and visual feedback rates, the R2R communications rates, and the U2R commands rates are allocated.

Hence, the elements of X are defined as follows:

- x1: Rate of visual feedback from R1
- x2: Rate of haptic feedback from R1
- x3: Rate of visual feedback from R2

• x4: Rate of haptic feedback from R2

• x5: Rate of R2R collaboration information exchange

• x6: Rate of commands generation

The observations in pi's are also defined below:

• p1: Distance to obstacle from R1

• p2: Distance to obstacle from R2

• p3: Speed of formation (Combined from R1 and R2)

• p4: Positioning error in the horizontal direction Δx

• p5: Positioning error in the vertical direction Δy.

• p6: Personalizing factor

Moreover, as mentioned above that each element of P is normalized with respect to the maximum value of the corresponding observation.

Hence below p1 and p2 are defined to be normalized with respect to the maximum distance value detectable by the sensor of the robot which is 200 cm:

$$p1 = (200 - \ Distance\ from\ R1)/200 \quad (4)$$

$$p2 = (200 - \ Distance\ from\ R2)/200 \quad (5)$$

Also p3 is defined as follows considering v1 and v2 to be the average forward/backward and sideway speed of the formation, respectively, where the maximum sideway and forward speed reached by the robots are 10cm/s and 50 cm/s, respectively:

$$p3 = \frac{\sqrt{{v_1}^2 - {v_2}^2}}{\sqrt{{v_{1max}}^2 - {v_{2max}}^2}} \quad (6)$$

Where $v_{1max} = 50\ cm/s$ and $v_{2max} = 10\ cm/s$

Furthermore, below p4 and p5 are defined to be normalized with respect to the maximum position error in the vertical direction (Δy) and in the horizontal direction (Δx):

$$p4 = \min(\frac{|e_x|}{e_{xmax}}, 1) \quad (7) \qquad p5 = \min(\frac{|e_y|}{e_{ymax}}, 1) \quad (8)$$

Knowing that the maximum position error allowed in the vertical and horizontal directions $e_{ymax}$ and $e_{xmax}$ for this specific task are respectively 1 cm and 5 cm.

Besides, p6 is defined to represent the PF upon the teleoperation task; this is done through monitoring the presence or the absence of the distraction encountered by the operator through the collaboration task. Thus p6 is set to be 0 in the case of no distraction and 1 in the case of distraction presence, where the determination and the sensing of the accurate level of disturbance is beyond this research scope considering that the focus here is to build an operator-based bandwidth management scheme that can rely on several sensing mechanisms to obtain the PF corresponding value.

Figure 5 shows an overview of the designed dynamic bandwidth algorithm, which takes as input the performance measures from the robots (representing PF, IEs and QoC) and determines accordingly the real-time distribution of the available

bandwidth among the R2U, R2R and U2R communication channels in a way to optimize performance and determine the appropriate real-time bandwidth rates Xs.

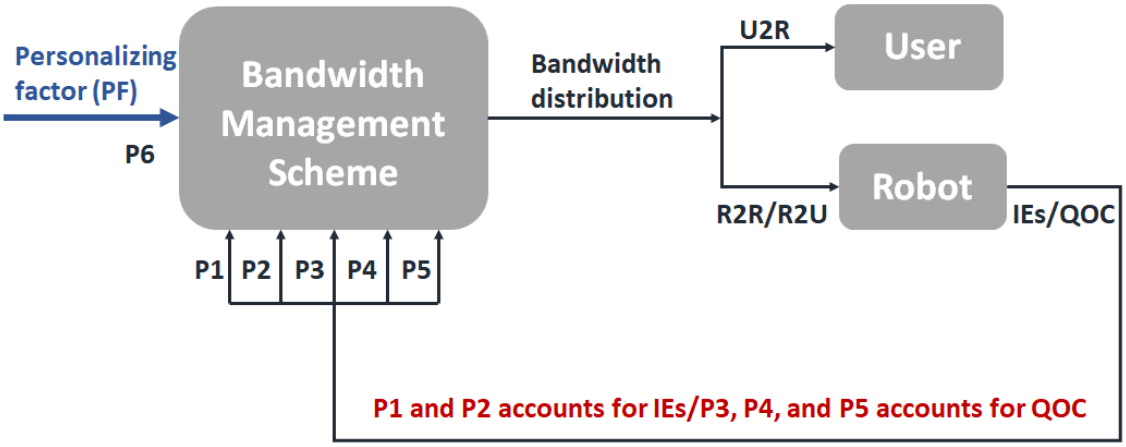


*Figure 5 Operator-Based Dynamic Bandwidth Management scheme*

Below is the corresponding relation between the set of rates Xs and the set representing the various observations Ps:

$$P = \begin{bmatrix} P1 \\ P2 \\ . \\ . \\ . \\ Pm \end{bmatrix} = \begin{bmatrix} IE \\ QoC \\ PF \end{bmatrix} \quad (2) \qquad X = \begin{bmatrix} x1 \\ x2 \\ . \\ . \\ . \\ xr \end{bmatrix} = M\,P \quad (2)$$

**P1 and P2 account for IEs**

**P3, P4 and P5 account for QOC**

**P6 represents the PF, it accounts for disturbance presence/absence**

Moreover, knowing that M is a 6x6 matrix representing the weights for the corresponding performance measures (P values); thus, it should dynamically adapt to

the IEs, QoC and the PF to increase the efficiency and optimality of this operator-based bandwidth management scheme to determine the appropriate real-time bandwidth rates Xs. Hence the corresponding M matrix has to change values accordingly to adapt with the various changes

within the tele-operation task, so that the bandwidth management is optimized in real-time considering the corresponding task conditions at each point in time. So, a two-level controller is implemented in the section below to determine the appropriate M matrix in real-time.

## 3.4 Two-level controller solution of the optimization problem

This section presents the implementation of the designed two-level controller over the teleoperation application described above.

### 3.4.1 *M matrix Division into Clusters/Groups*

In our application we formed four distinct groups, depending on the intuition and application heuristics, as shown in figure 6 below:

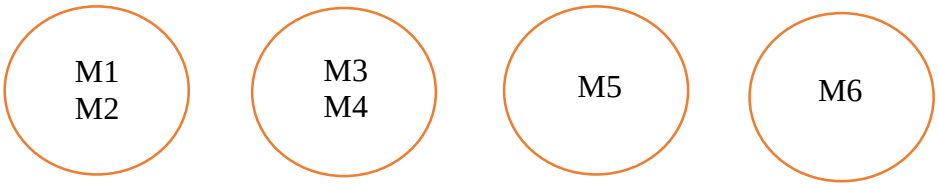


*Figure 6 M matrix grouping*

- M1 and M2 are the rows of the M matrix which corresponds to the rates of the visual and haptic feedback of R1 respectively [Robot to User, R2U rates].

- M3 and M4 are the rows of the M matrix which corresponds to the rates of the visual and haptic feedback of R2 respectively [Robot to User, R2U rates].
- M5 is the row of the M matrix which corresponds to the rates of the R2R collaboration information exchange [Robot to Robot, R2R rates].
- M6 is the row of the M matrix corresponding to the rate of commands generation [User to Robot, U2R rates].

### 3.4.2 *Qualitative Rules Generation*

Each group of rates has dependences on its corresponding performance measures [P] only, in a way to optimize the M matrix weights distribution; non-dependence is represented by 0 in the corresponding M matrix entry.

- G1: Is mainly affected by P1, P3 and P6 [feedback from R1 not affected by the distance to obstacle of R2 or the positioning error]
- G2: Is mainly affected by P2, P3 and P6 [feedback from R2 not affected by the distance to obstacle of R1or the positioning error]
- G3: Is mainly affected by P4 and P5 [Rate of information exchange is mainly affected by the positioning errors]
- G4: Is mainly affected by P1, P2, P3 and P6 [rate of command generation is affected by the distance to obstacle of both R1 and R2 along with the Speed of formation (QoC) and personalizing factor].

### 3.4.3 *Fuzzy Logic Controller Design*

- Fuzzification: this is the process where qualitative measures/rules inputs are transformed and classified into possible fuzzy sets, taking into consideration the full domain of each variable. Hence within this state a certain type of membership function is developed over various input variables.
  Furthermore, a serious identification of qualitative measures/rules inputs is required and pre-requisite to transform these qualitative measures into quantitative measures where all available inputs are stated and classified.

  Since the values for the P factors are normalized between 0 and 1, we will consider three ranges for each of the P factors; noticing the sensitivity of each performance measure and the corresponding importance to be given to this P value while forming the constraints of the optimization algorithm:

  - L: Low; [0, 0.4[ region

  - M: Medium; [0.4, 0.7[ region

  - H: High; [0.7, 1] region

### 3.4.4 *Level 2 Constraints Generation*

- Inference rules: this is the process which relates the resulting input membership functions [set through the fuzzification process] and the suitable output weights for the M matrix, depending on application heuristics. Thus a series of "If-then" statements is developed presenting the established fuzzy relations between the fuzzy set inputs developed in part 1 and the appropriate weights for the M matrix output. Moreover, for the ease of decision and implementation and to avoid

dealing with a huge number of combinations, the processes of setting inference rules is accomplished using layering along with divide and concur techniques. This stage considers all possible combinations of the input values and scatters them into groups according to the ones which result in the same output values [the appropriate set of constraints]. Considering that the input-output relationship will be as follows:

L corresponds to 3

M corresponds to 2

H corresponds to 1

Example if input of a group is (H, M, L) then the corresponding constraint will be:

$$X_1 + 2X_2 + 3X_3 = 1 \quad (9)$$

De-fuzzification: this is the process which links each group of combinations developed by the inference rules to the appropriate set of constraints to be fed to the optimization level 2 control. Moreover, the defuzzified output consist of a set of 6 constraints [each corresponding to a row of the M matrix; considering that the sum of each row's inputs will be 1] which will specify the appropriate guidance for the optimization algorithm to consider in its update. In addition, this step will be done for each of the 4 groups separately at this stage [may be combined later].

G1: Is mainly affected by P1, P3 and P6; so considering the ranges we have 27 possible combinations and will be mapped into the appropriate constraint as mentioned before.

G2: Is mainly affected by P2, P3 and P6; so considering the ranges we have 27 possible combinations and will be mapped into the appropriate constraint as mentioned before.

G3: Is mainly affected by P4 and P5; so considering the ranges we have 9 possible combinations and will be mapped into the appropriate constraint as mentioned before.

G4: Is mainly affected by P1, P2, P3 and P6; so considering the ranges we have 81 possible combinations and will be mapped into the appropriate constraint as mentioned before.

Thus the designed fuzzy logic controller will be implemented through 144 if-then statements which represent the inference rules and link the appropriate optimization constraints to the current set of P inputs [performance measures].

### 3.4.5 *Lagrange Optimization Design*

To implement the Lagrange based optimization algorithm [Level 2 controller] we need a cost function and a set of constraints; thus the optimization scheme will minimize the cost function following the required constraints.

In our application we will be considering the bandwidth optimization cost function (3) where Wi reflects the corresponding overhead of each feedback stream on the bandwidth consumption.

$$\sum_{i=1}^{r} w_i x_i - B_{max} \leq 0 \qquad (3)$$

knowing that the sum of inputs of each row of the M matrix is 1.

Thus we will use this fact to derive the following set of constraints [this will be derived from the output of the fuzzy logic level 1 controller, considering the distinguished groups and their dependences]. This will lead to a set of four constraints [each corresponding to a group of the M matrix rows] which will enable the optimization scheme to adapt according to the guidance of the level 1 controller. The set of constraints will be, for example:

$$X_1 + 2X_2 + 3X_3 = 1 \quad (9)$$

$$3X_4 + 2X_5 + 3X_6 = 1 \quad (10)$$

$$2X_7 + 3X_8 = 1 \quad (11)$$

$$2X_9 + 2X_{10} + 2X_{11} + 3X_{12} = 1 \quad (12)$$

Where $X_i$s corresponds to different interties of the M matrix which are updated in real-time corresponding to the required adaptation with the current system status.

Moreover, we need to transform our cost function (3), to an equation in terms of the real time variable $X_i$s which can be coded to be solved continuously to adapt with the real-time change in the system status.

Thus $\sum_{i=1}^{r} \mathbf{w_i x_i}$ is transformed to the following equation:

$$
\begin{aligned}
&W_1[X_1P_{1+}X_2P_{3+}X_3P_6] + W_2[X_1P_{1+}X_2P_{3+}X_3P_6] + W_3[X_4P_{2+}X_5P_{3+}X_6P_6] + \\
&+W_4[X_4P_{2+}X_5P_{3+}X_6P_6] + W_5[X_7P_{4+}X_8P_5] + W_6[X_9P_{1+}X_{10}P_{2+}X_{11}P_3 + X_{12}P_6] \\
&= [W_1 + W_2]\,[X_1P_{1+}X_2P_{3+}X_3P_6] + [W_3 + W_4][X_4P_{2+}X_5P_{3+}X_6P_6] + W_5[X_7P_{4+}X_8P_5] + \\
&W_6[X_9P_{1+}X_{10}P_{2+}X_{11}P_3 + X_{12}P_6] \\
&= [(W_1 + W_2)P_1]X_1 + [(W_1 + W_2)P_3]X_2 + [(W_1 + W_2)P_6]X_3 + [(W_3 + W_4)P_2]X_4 + \\
&[(W_3 + W_4)P_3]X_5 + [(W_3 + W_4)P_6]X_6 + [W_5P_4]X_7 + [W_5P_5]X_8 + [W_6P_1]X_9 + \\
&[W_6P_2]X_{10} + [W_6P_3]X_{11} + [W_6P_6]X_{12}
\end{aligned}
\tag{33}
$$

This will be fed to the optimization scheme and the M matrix entries will be calculated continuously to adapt with the real-time change in the system status [coded in MATLAB, and Linprog solver is used considering it's fit to the proposed task].

### 3.4.6 *Bandwidth Rates Determination*

The implemented optimization scheme will consider the bandwidth management cost function and the real time obtained constraints set from the fuzzy level 1 controller to obtain the appropriate values for the M matrix entries in a manner to adapt with the system status. Then we will use these entries to determine the real time bandwidth rates [first output of the level 2 controller] as follows:

$$R1 = X_1*P_1 + X_2*P_3 + X_3*P_6 \tag{14}$$

$$R2 = X_1*P_1 + X_2*P_3 + X_3*P_6 \tag{15}$$

$$R3 = X_4*P_2 + X_5*P_3 + X_6*P_6 \tag{16}$$

$$R4 = X_4*P_2 + X_5*P_3 + X_6*P_6 \tag{17}$$

$$R5 = X_7 * P_4 + X_8 * P_5 \quad (18)$$

$$R6 = X_9 * P_1 + X_{10} * P_2 + X_{11} * P_3 + X_{12} * P_6 \quad (19)$$

Then these obtained rates will be used to calculate the corresponding used bandwidth at this state as follows:

$$\begin{aligned} \sum_{i=1}^{r} \mathbf{w_i x_i} = {} & W_1[X_1P_{1+}X_2P_{3+}X_3P_6] + W_2[X_1P_{1+}X_2P_{3+}X_3P_6] + \\ & W_3[X_4P_{2+}X_5P_{3+}X_6P_6] + W_4[X_4P_{2+}X_5P_{3+}X_6P_6] + \\ & W_5[X_7P_{4+}X_8P_5] + W_6[X_9P_{1+}X_{10}P_{2+}X_{11}P_3 + X_{12}P_6] \end{aligned} \quad (20)$$

To ensure that the cost function (3) is satisfied, where:

W = [460800 12000 460800 12000 24000 24000] and Bmax = 1.4 Mbps.

Note: the designed two-level controller is compatible with the case where the maximum available bandwidth varies throughout the teleoperation task, and is capable of determining the optimal distribution of the real-time Bmax.

# CHAPTER 4

# SIMULATION & RESULTS

## 4.1 Preamble

The simulation section presents first the validation simulation conducted over MATLAB, this simulation considers two various cases: one with disturbance presence and the other without disturbance. In addition, the simulation section presents the scaling scheme simulation conducted over WEBOTS.

## 4.2 MATLAB validation simulation

For the sake of evaluating the operator-based bandwidth management algorithm, a MATLAB validation simulation is implemented; where the operator-based bandwidth management algorithm is tested against the optimized rates algorithm presented by Mansour et al. [1, 2].

During the simulations, participants are required to control the 2 humanoid robots through a predefined track while avoiding the track obstacles. The task will be done over traditional bandwidth method and the novel two-level control method for the bandwidth division with differentiating two cases for each method, one with disturbance presence and one without disturbance; where the disturbance is considered to be noisy music. This testing scenario was implemented such that the operator controls the movements of the two robots through a haptic joystick in a way to avoid the obstacles throughout the path. Figure 7 below shows a sample of the simulator testing, where the

two controlled robots are presented by the red and the blue circles and the obstacles are presented by the two green circles. Moreover, the tele-operation task consists of driving the robots within the path specified by the dashed green line.

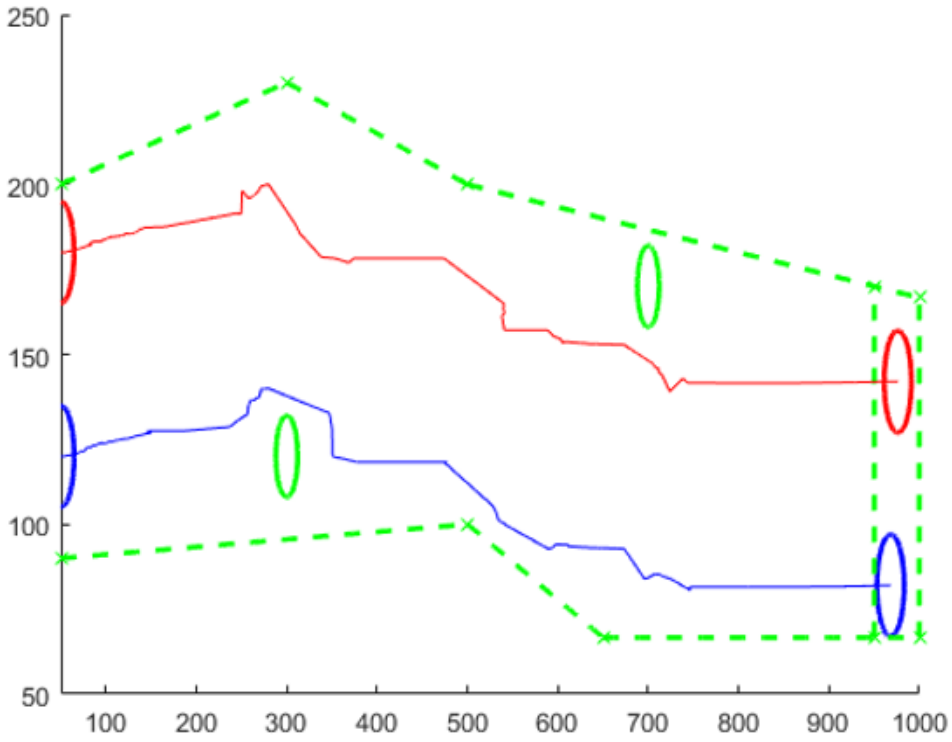


*Figure 7 Sample of the conducted tele-operation task*

In order to evaluate the suggested algorithm 5 teleoperators were randomly chosen to drove the swarm under the proposed two-level controller method and Optimized Bandwidth method presented in [1]. Each teleoperator drives the swarm under both algorithms with two various cases: disturbance presence and absence and each scenario is executed twice by the operator; thus in total each operator executes eight different trials, where the order of the trials is chosen randomly through flipping a coin. In each trial, the following performance parameters are collected: the duration of

the task in seconds, the distance covered by each robot in mm, the exit distance in mm of each robot from the specified path, the exit time in seconds of each robot from the specified path, the corresponding average distance to obstacle (DTO) in mm from each robot, the average horizontal error in the specified alignment of the robots in mm, the average vertical error in the specified alignment of the robots in mm, and the average used bandwidth in bps. It is worth mentioning that the consumed bandwidth is computed using the known image frame size of the used cameras as well as the other data exchanged sizes. The conducted simulations result of the disturbance presence scenario are presented in Table 1 and that of disturbance absence in Table 2.

### 4.2.1 *MATLAB Disturbance Presence Results*

Table 1 presents the MATLAB results summary for the disturbance presence scenario.

*Table 1 MATLAB simulation disturbance presence scenario results*

| | | Duration (sec) | DistR1 (mm) | DistR2 (mm) | Exit DistR1 (mm) | Exit DistR2 (mm) | Exit TimeR1 (sec) | Exit TimeR2 (sec) | Average DTO1 (mm) | Average DTO2 (mm) | Average HorError (mm) | Average VerError (mm) | Average Bw (bps) |
|---|---|---|---|---|---|---|---|---|---|---|---|---|---|
| Optimized rates | Average | 34.987 | 1127 | 1121 | 53.091 | 20.266 | 1.773 | 0.742 | 192.719 | 185.128 | 8.81 | 0.70 | 953605 |
| | Standard Deviation | 3.117 | 44.9 | 75.46 | 26.065 | 10.497 | 0.875 | 0.618 | 3.919 | 2.407 | 0.59 | 0.08 | 8890.2 |
| Operator Aware | Average | 27.099 | 1101 | 1098 | 49.81 | 5.048 | 1.68 | 0.25 | 190.943 | 182.547 | 5.17 | 0.42 | 747938 |
| | Standard Deviation | 2.241 | 35.65 | 73.24 | 21.58 | 2.54 | 0.54 | 0.134 | 3.456 | 2.148 | 0.49 | 0.07 | 6775.3 |
| | Percentage Difference Optimized - Operator | **25.401** | **2.334** | **2.073** | **6.377** | **120.233** | **5.387** | **99.194** | **0.926** | **1.404** | **52.074** | **50** | **24.174** |

Table 1 shows that the operator aware bandwidth management algorithm has better performance compared to the optimized rates algorithm in the case of disturbance

presence. The conducted results show that the operator aware algorithm requires 25.401% less execution time and 24.174% less used bandwidth for the task execution. Moreover, table 1 shows the superiority of the operator aware algorithm in terms of the covered distance by both robots in addition to the average distance to obstacle (DTO) measured by both robots; as well as the exit time and exit distance.

### 4.2.2 *MATLAB Disturbance Absence Results*

Table 2 presents the MATLAB results summary for the disturbance absence scenario.

*Table 2 MATLAB simulation disturbance absence scenario results*

| | | Duration (sec) | DistR1 (mm) | DistR2 (mm) | Exit DistR1 (mm) | Exit DistR2 (mm) | Exit TimeR1 (sec) | Exit TimeR2 (sec) | Average DTO1 (mm) | Average DTO2 (mm) | Average HorError (mm) | Average VerError (mm) | Average Bw (bps) |
|---|---|---|---|---|---|---|---|---|---|---|---|---|---|
| Optimized rates | Average | 29.541 | 1100 | 1109 | 46.124 | 16.324 | 0.686 | 0.243 | 96.197 | 92.982 | 6.18 | 0.21 | 873645 |
| | Standard Deviation | 2.316 | 41.2 | 70.26 | 13.586 | 5.853 | 0.0586 | 0.081 | 2.405 | 1.782 | 0.49 | 0.053 | 5432.6 |
| Operator Aware | Average | 25.158 | 1207 | 1187 | 58.724 | 2.804 | 0.86 | 0.17 | 100.394 | 98.4003 | 4.98 | 0.31 | 687432 |
| | Standard Deviation | 1.057 | 32.83 | 63.42 | 11.24 | 0.45 | 0.029 | 0.056 | 1.683 | 1.048 | 0.35 | 0.025 | 5321.5 |
| | Percentage Difference Optimized - Operator | **16.025** | **-9.276** | **-6.794** | **-24.03** | **141.363** | **-22.509** | **35.351** | **-4.27** | **-5.662** | **21.505** | **-38.462** | **23.856** |

Table 2 shows that the operator aware algorithm requires 16.025% less execution time and 23.856% less used bandwidth for the task execution. Moreover, table 2 shows that the operator aware algorithm has better performance for some factors and the optimized rates algorithm has better performance in terms of the other factors for this conducted disturbance absence scenario.

## 4.3 WEBOTS scaling simulation

For the sake of showing the scalability of the designed operator-based bandwidth management algorithm, the implemented two-level controller is integrated into a WEBOTS simulation to show that this algorithm can be integrated into more complex teleoperation tasks; where the operator-based bandwidth management algorithm is tested against the optimized rates algorithm presented by Mansour et al. [1, 2].

The implemented simulation requires the operator to control 10 Nao robots through a predefined track while avoiding the track obstacles. The task is done over traditional bandwidth method and the proposed two-level control method for the bandwidth division differentiating two cases for each method, one with disturbance presence and one without disturbance; where the disturbance is considered to be noisy music. This testing scenario is implemented such that the operator controls the movements of the integrated robots through a haptic joystick in a way to avoid the obstacles throughout the path. Figure 8 below show the WEBOTS testing setup; which shows the 10 humanoid robots integrated in the teleoperation task along with their predefined path to follow. Moreover, the tele-operation task consists of driving the robots within the path specified while avoiding any obstacle within this path.

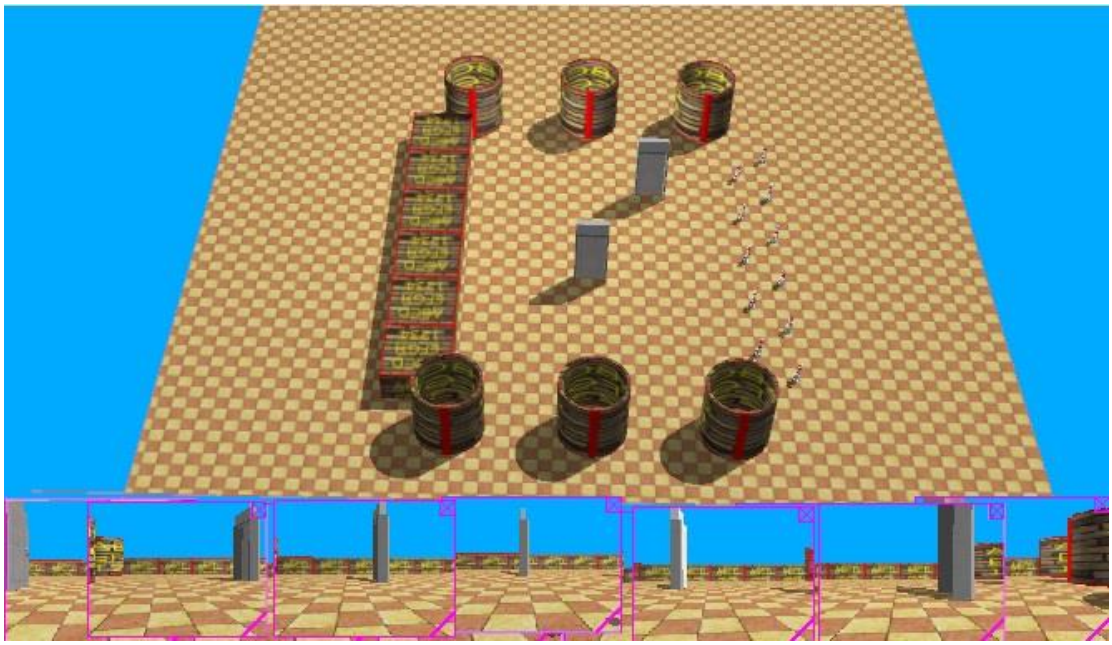

*Figure 8 WEBOTS Testing Setup overview*

The designed WEBOTS testing setup targets the collaboration of 10 Nao humanoid robots for the sake of completing a teleoperation task; the task is to drive the swarm of the robots using a haptic feedback joystick through the specified path from a predefined set point into a well-known end point while avoiding the track obstacles as shown in figure 9 below.

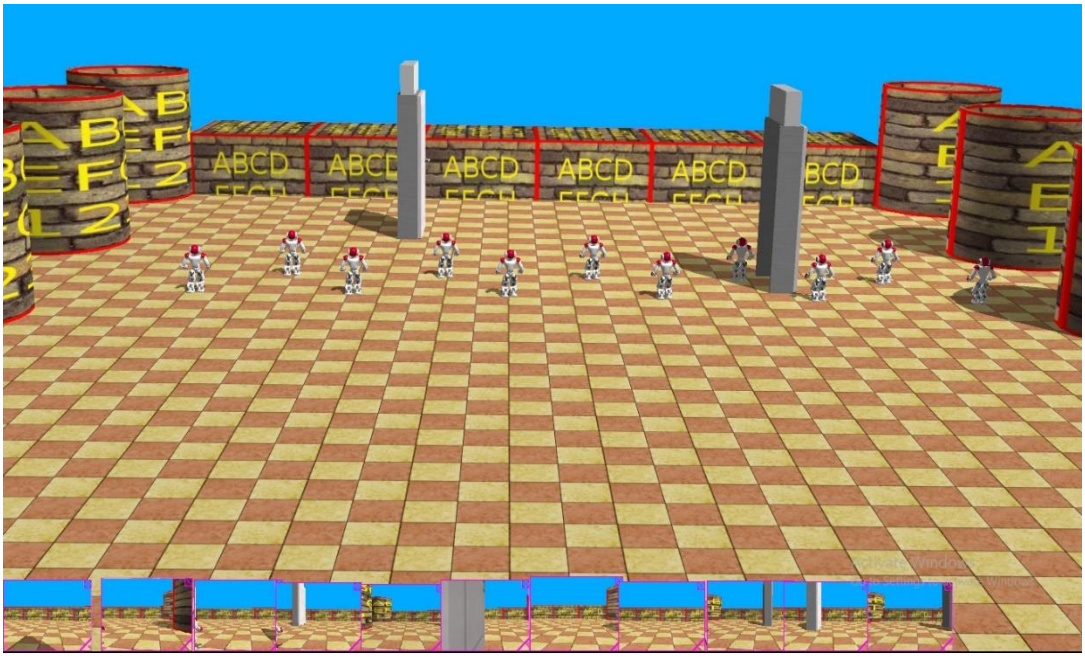


*Figure 9 Sample of the conducted WEBOTS Testing*

During this simulation the swarm is driven under the proposed two-level controller method and Optimized Bandwidth method presented in [1] under the scenario of disturbance presence as well as disturbance absence; upon each trial the following performance parameters are collected: the duration of the task in seconds, the average distance covered by robots in mm, the average exit distance in mm from the specified path, the average exit time in seconds from the specified path, the corresponding average distance to obstacle (DTO) in mm, the average horizontal and vertical error in the specified alignment of the robots in mm, and the average used bandwidth in bps. It is worth mentioning that the consumed bandwidth is computed using the known image frame size of the used cameras as well as the other data exchanged sizes. The conducted simulations result of the disturbance presence scenario are presented in Table 3 and that of disturbance free scenario in Table 4.

### 4.3.1 *WEBOTS Disturbance Presence Results*

Table 3 presents the WEBOTS results summary for the disturbance presence scenario.

*Table 3 WEBOTS simulation disturbance presence scenario results*

| | | Duration (sec) | Distance (mm) | Exit Distance (mm) | Exit Time (sec) | Average DTO (mm) | Average HorError (mm) | Average VerError (mm) | Average Bw (bps) |
|---|---|---|---|---|---|---|---|---|---|
| Optimized rates | Average | 120.86 | 3276.00 | 19.64 | 7.68 | 216.86 | 14.68 | 0.68 | 1345967.00 |
| | Standard Deviation | 13.49 | 73.68 | 5.82 | 1.13 | 5.82 | 0.84 | 0.05 | 8763.80 |
| | Percentage | 0.53 | 0.52 | 0.69 | 0.55 | 0.52 | 0.63 | 0.64 | 0.53 |
| Operator Aware | Average | 107.36 | 3021.00 | 8.64 | 6.23 | 196.38 | 8.75 | 0.39 | 1198345.00 |
| | Standard Deviation | 2.24 | 56.83 | 2.34 | 0.35 | 4.91 | 0.46 | 0.04 | 7645.48 |
| | Percentage | 0.47 | 0.48 | 0.31 | 0.45 | 0.48 | 0.37 | 0.36 | 0.47 |
| | Percentage Difference Optimized - Operator | **11.83** | **8.10** | **77.79** | **20.85** | **9.91** | **50.62** | **54.21** | **11.60** |

Table 3 shows that the operator aware bandwidth management algorithm has better performance as compared to the optimized rates algorithm in the case of disturbance presence. The conducted results show that the operator aware algorithm requires 11.83% less execution time and 11.6% less used bandwidth for the task execution. Moreover, table 3 shows the superiority of the operator aware algorithm in terms of the average covered distance by robots in addition to the average distance to obstacle (DTO) measured by robots; as well as the exit time and exit distance.

### 4.3.2 *WEBOTS Disturbance Absence Results*

Table 4 presents the WEBOTS results summary for the disturbance absence scenario.

*Table 4 WEBOTS simulation disturbance absence scenario results*

| | | Duration (sec) | Distance (mm) | Exit Distance (mm) | Exit Time (sec) | Average DTO (mm) | Average HorError (mm) | Average VerError (mm) | Average Bw (bps) |
|---|---|---|---|---|---|---|---|---|---|
| Optimized rates | Average | 106.86 | 3127.00 | 14.20 | 6.73 | 197.42 | 11.53 | 0.57 | 1246734.00 |
| | Standard Deviation | 10.57 | 67.83 | 4.62 | 1.02 | 4.73 | 1.14 | 0.04 | 8235.67 |
| Operator Aware | Average | 98.53 | 3045.00 | 11.73 | 5.87 | 192.36 | 10.24 | 0.37 | 1143562.00 |
| | Standard Deviation | 2.18 | 54.68 | 3.98 | 0.28 | 4.57 | 0.96 | 0.03 | 7538.67 |
| | Percentage Difference Optimized - Operator | **8.11** | **2.66** | **19.05** | **13.65** | **2.60** | **11.85** | **42.55** | **8.63** |

The operator aware bandwidth management algorithm proves its improved performance over the optimized rates algorithm in the case of disturbance absence as well. The conducted results show that the operator aware algorithm requires 8.11% less execution time and 8.63% less used bandwidth for the task execution. Moreover, table 4 shows the superiority of the operator aware algorithm in terms of the average covered distance by robots in addition to the average distance to obstacle (DTO) measured by robots; as well as the exit time and exit distance.

# CHAPTER 5

# EXPERIMENTAL SETUP AND RESULTS

## 5.1 Preamble

Chapter 5 presents the system parts description which considers the used NAO humanoid robots along with their corresponding sensors. After that, the experimental setup is presented followed by the implemented testing scenarios. This chapter is concluded by presenting the experimental objective and subjective results.

## 5.2 System Description

The following paragraph provides a description of the experiment designed to achieve the research goal. The experiment is designed to be used with a force feedback joystick (Microsoft SideWinder Force Feedback 2) shown in figure 10, which is a standard gaming joystick, to navigate two humanoid robots (figure 11) through a delimited path to reach a predetermined destination while avoiding obstacles and preserving a formation (60 cm that separates the two robots in the horizontal direction while being aligned along the vertical direction). Also, each robot provides the operator with the adequate visual feedback through transmitting real-time video streaming; considering that the operator is not aware about the path and this visual feedback is what makes the operator informed about the formation motion. Besides, the R2R information exchange rate will enable exchanging the relative real-time positions of the 2 robots to know the formation status and activate the automatic obstacle avoidance algorithm. In the case where the distance to obstacle for any of the swarm's robots is less than the minimum

accepted distance the swarm will immediately stop and preserves its current formation.

*Figure 10 Microsoft SideWinder Force Feedback 2 joystick*

*Figure 11 Humanoid Robots Experimental Setup*

The used Nao robot in the conducted experiments as well as its sensors are first described, then the accompanied experiments are discussed and analyzed, and the corresponding conclusions are shown.

### 5.2.1 *NAO Humanoid Robots*

Nao, shown in Figure 12, is a programmable, 58cm tall, with a body characterized by 25 degrees of freedom (DOF) with main components being actuators and electric motors. Nao has an integrated sensor network, containing sonar rangefinder, cameras, microphones, IR emitters and receivers, an inertial board, along with pressure and tactile sensors. Nao similarly contains an Intel ATOM 1.6Ghz CPU (located in Nao's head) which runs a Linux kernel and supports Aldebaran's proprietary middleware platform. Nao is power-driven by a 27.6-watt-hour battery which offers it autonomy of about 1 hour, depending on usage. To drive Nao, the previously mentioned force feedback joystick (Microsoft SideWinder Force Feedback2) is used to send Forward/Backward level controlling commands in real-time, Brake level as well as Steering level.

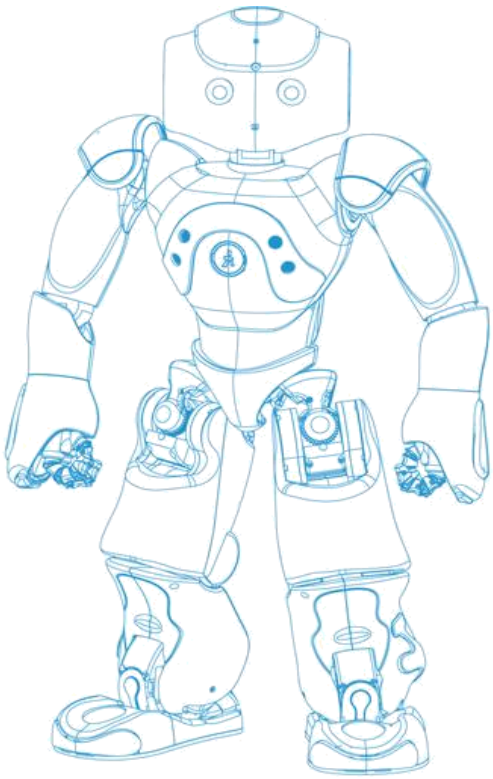

*Figure 8 NAO Humanoid Robot*

### 5.2.2 *Sensory Readings*

The used NAO robot has two cameras and two ultrasonic sensors pairs (Figure 13) positioned on the robot's front. The ultrasonic sensors can detect measurements in the range between 2.5 and 0.2 m, specifying the distance to the nearby obstacle in meters. In the case where the distance is greater than or equal to 250cm, or less than or equal to 20cm, the sensor respectively then returns the value 2.5 and 0.2 m; else, the value returned is in the corresponding sensor's range. Moreover, these distance to obstacle measures are the only source of the haptic feedback offered to the operator throughout the teleoperation task. Besides, the 2 two 920p available cameras can capture up to 30 images/second and can track, acquire, and identify faces and images. The first camera, positioned at mouth level, images the direct surroundings, whereas the second positioned on NAO's forehead images the horizon.

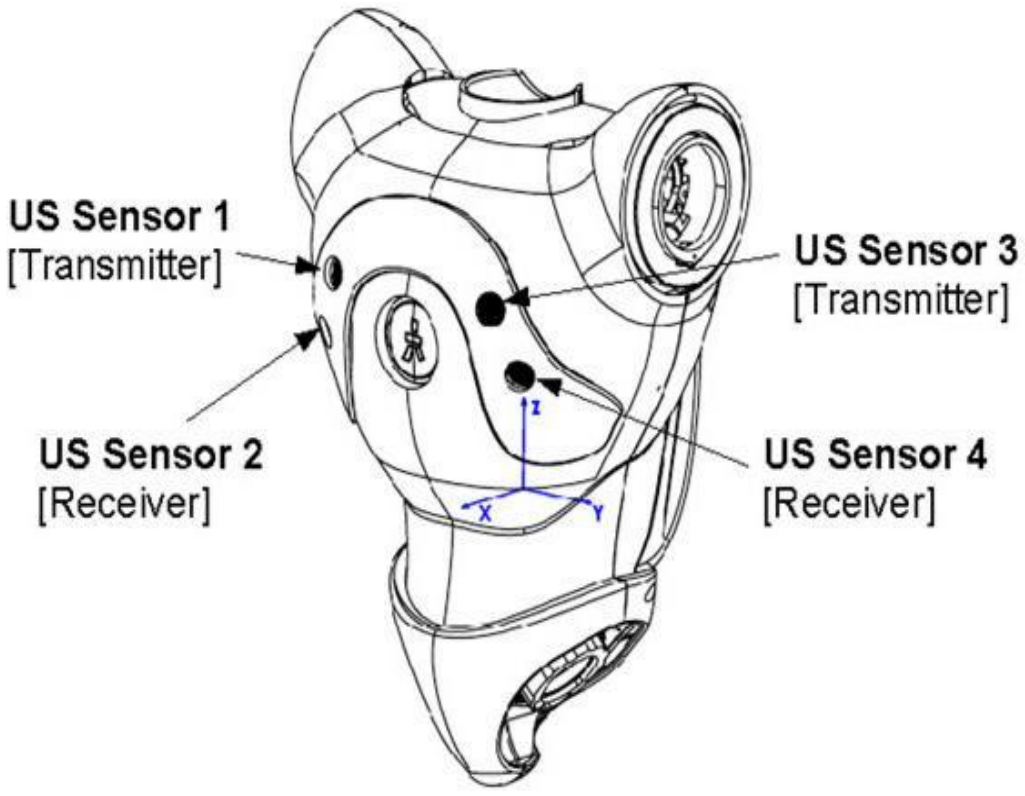


*Figure 13 Ultrasonic sensors pairs*

## 5.3 **Experimental Setup**

For the sake of controlling the corresponding robots' swarm a TCP/IP communication channel is established between the MATLAB implementation of the novel 2 level controller (which takes the U2R commends as inputs) and the python code which receives the R2U feedback channels as shown in the below image.

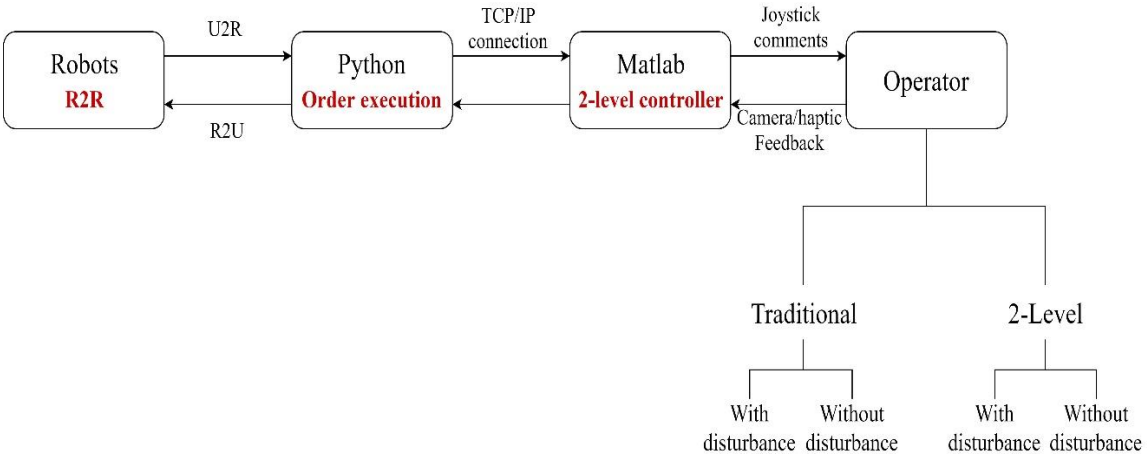


*Figure 9 Communication scheme*

Moreover, the performed experiments are done in the UAV room in the Vision and Robotics Lab facilities where the operator is isolated visually from the robots performing the task; thus the operator will be in the control zone upon executing the teleoperation task, while the robots will be in the testing zone and the operator will be totally isolated from hearing/seeing the robots as shown in the below image.

*Figure 10 Experimental Setup*

Besides, all the conducted experiments are monitored through Optitrack motion capture system to analyze and compare the performance of both algorithms under the 2 described scenarios.

## 5.4 **Testing Scenarios**

During the experiment, participants are required to control the two humanoid robots through a predefined track while avoiding the obstacles as shown in figure 16 below; this task will be done over traditional bandwidth method and the novel two-level control method for the bandwidth division while differentiating two cases for each method, one with disturbance presence and one without disturbance. The task took around 30 minutes for each participant and disturbance is done through Delayed Digital Recall (n-back) task. This method developed by the MIT AgeLab increases the cognitive demand placed on an individual. The lab has used this task in a series of driver workload and distraction studies [36].

*Figure 11 Humanoid Robots' path and alignment*

It is not a binary operation to pay attention to the road, the operator will have variable attention degrees depending on his/her focus on the driving task. This attention variation is simulated through 0, 1, and 2- back tasks model developed by the MIT AgeLab, the task will decrease the attention to scanning the roadway through increasing the cognitive load levels. Thus this task is intended to simulate what will the individual face throughout the driving experience, such as phone conversation. The Delayed Digit Recall n-back task is currently being used in the International Standard Organization's (ISO) TC22/SC13/WG 8 project, Coordinated Studies on the Detection Response Task (DRT), as a surrogate for cognitive demand. Studies are taking place in Germany, France, Sweden, Canada, China and the United States.

Below are the detailed steps followed for each participant engaged in this testing:

1. Each research subject enters first the VRL room and is informed that the research proposes no more than the minimal risk and is instructed on how to contact the IRB office if adverse events occur, as they have been provided by the

name and phone number of MD. Fuad Ziyadeh, chairperson of the Social and Behavioral Sciences IRB.

2. The participant is then asked to sign the consent form and is asked the following questions:

   - If he/she is left/right handed

   - If he/she has an experience in gaming

   - If he/she has an experience in Teleoperation

   These data are saved as part of comparing both bandwidth management algorithms.

3. The participant is given then an explanation about the experiment and that he/she will have a bulk of eight trials where each trial will require around 3 min so in total the experiment will take around 30 min, and is informed about the different parts of the system and the difference between the case with disturbance and without disturbance. Moreover, the participant experience first a training trial at this stage before continuing the experiment so that they get familiar with the experiment setup and get used to the various experimental parts.

4. The participant is then asked to flip a coin twice to randomly choose between the four possible combinations of the trials:

   - 1/D 2/D 1/ND 2/ND corresponds to tail/tail

   - 2/D 1/D 2/ND 1/ND corresponds to tail/head

   - 1/ND 2/ND 1/D 2/D corresponds to head/tail

- 2/ND 1/ND 2/D 1/D corresponds to head/head

Where 1 stands for the traditional dynamic bandwidth management method, stands for the two-level control for the bandwidth management with accounting for personalizing factor, D stands for disturbance presence, and ND stands for disturbance absence.

5. Perform the four trials and the data collected will be stored in Microsoft Excel files on an AUB password protected computer. In addition, the data collected is anonymous, the file name and the data stored will not allow participant identification. The data is stored till the end of the study.
6. Repeat steps 4 and 5.

The collected data are: the duration of the task in seconds, the distance covered by each robot in mm, the exit distance in mm of each robot from the specified path, the exit time in seconds of each robot from the specified path, the corresponding average distance to obstacle (DTO) in mm from each robot, the average horizontal error in the specified alignment of the robots in mm, the average vertical error in the specified alignment of the robots in mm, and the average used bandwidth in bps.

Participants are participating voluntarily and without any financial benefits, however, they were made aware of the contribution they are providing to this research field and its various applications. Furthermore, participants were asked to fill the attached NASA Task Load Index form for each conducted trial; this form is used to assess their subjective perception of the driving.

## 5.5 Experimental Execution & Results

This section presents the obtained subjective results from the used NASA Task Load Index form along with the objective results obtained from the Optitrack motion detection system for both methods under the two conducted scenarios. These results are collected from the participation of 15 testing subject in the stated experiment procedure. The task was performed by a group of 15 Participant with the below characteristics:

- Age: between 22 and 31 years
- 5 females and 10 males
- 14 right handed and 1 left handed
- 14 has previous experience in gaming
- 5 has previous experience in teleoperation

### 5.5.1 *Experimental Disturbance Presence Results*

Table 5 presents the experimental results summary for the disturbance presence scenario.

*Table 5 Experimental disturbance presence scenario results*

| | | Duration (sec) | DistR1 (mm) | DistR2 (mm) | Exit DistR1 (mm) | Exit DistR2 (mm) | Exit TimeR1 | Exit TimeR2 | Average DTO1 (mm) | Average DTO2 (mm) | Average HorError (mm) | Average VerError (mm) | Average Bw (bps) |
|---|---|---|---|---|---|---|---|---|---|---|---|---|---|
| 1/D | Average | 29.263 | 1236 | 1219 | 49.526 | 18.243 | 1.548 | 0.698 | 189.654 | 179.346 | 9.463 | 1.246 | 987634 |
| | Standard Deviation | 2.584 | 50.6 | 60.4 | 22.476 | 9.146 | 0.736 | 0.487 | 3.145 | 2.135 | 0.678 | 0.13 | 8945.6 |
| | P value | 7.21 E-4 | 8.96 E-6 | 7.36 E-6 | 9.86 E-7 | 8.67 E-7 | 6.87 E-6 | 7.83 E-6 | 8.73 E-3 | 7.62 E-3 | 5.62 E-4 | 4.98 E-4 | 0.0135 |
| 2/D | Average | 24.168 | 1167 | 1157 | 42.59 | 4.873 | 1.24 | 0.24 | 178.269 | 172.364 | 5.016 | 0.418 | 736942 |
| | Standard Deviation | 1.756 | 34.59 | 38.67 | 19.57 | 3.672 | 0.48 | 0.124 | 2.876 | 1.879 | 0.3896 | 0.06 | 5462.2 |
| | P value | 6.94 E-4 | 8.26 E-6 | 6.94 E-6 | 9.74 E-7 | 8.25 E-7 | 6.79 E-6 | 7.68 E-6 | 7.96 E-3 | 7.43 E-3 | 5.28 E-4 | 4.63 E-4 | 0.0118 |
| | Percentage difference 1/D – 2/D | **19.071** | **5.743** | **5.219** | **15.059** | **115.677** | **22.095** | **97.655** | **6.189** | **3.970** | **61.427** | **99.519** | **29.073** |
| | Difference P value | **2.73 E-6** | **2.49 E-8** | **4.38 E-8** | **7.36 E-9** | **4.72 E-9** | **4.62 E-8** | **4.29 E-8** | **3.72 E-5** | **9.37 E-5** | **7.36 E-6** | **3.72 E-6** | **2.64 E-4** |

Table 5 shows that the operator aware bandwidth management algorithm has better performance as compared to the optimized rates algorithm in the case of disturbance presence. The conducted results show that the operator aware algorithm requires 19.071% less execution time and 29.073% less used bandwidth for the task execution. Moreover, table 5 shows the superiority of the operator aware algorithm in terms of the covered distance by both robots in addition to the average distance to obstacle (DTO) measured by both robots; as well as the exit time and exit distance.

### 5.5.2 *Experimental Disturbance Absence Results*

Table 6 presents the experimental results summary for the disturbance absence scenario.

*Table 6 Experimental disturbance absence scenario results*

| | | Duration (sec) | DistR1 (mm) | DistR2 (mm) | Exit DistR1 (mm) | Exit DistR2 (mm) | Exit TimeR1 | Exit TimeR2 | Average DTO1 (mm) | Average DTO2 (mm) | Average HorError (mm) | Average VerError (mm) | Average Bw (bps) |
|---|---|---|---|---|---|---|---|---|---|---|---|---|---|
| 1/ ND | Average | 26.578 | 1226 | 1198 | 46.35 | 15.68 | 1.468 | 0.673 | 176.346 | 172.364 | 8.964 | 1.167 | 926435 |
| | Standard Deviation | 2.672 | 40.983 | 53.69 | 18.34 | 8.346 | 0.6789 | 0.36 | 3.167 | 2.096 | 0.5963 | 0.12 | 8236.35 |
| | P value | 6.83 E-4 | 7.65 E-6 | 7.25 E-6 | 8.73 E-7 | 8.24 E-7 | 6.24 E-6 | 7.19 E-6 | 8.21 E-3 | 7.32 E-3 | 5.17 E-4 | 3.98 E-4 | 0.0114 |
| 2/ ND | Average | 22.436 | 1136 | 1096 | 37.42 | 4.35 | 1.137 | 0.23 | 167.346 | 163.649 | 4.837 | 0.409 | 729645 |
| | Standard Deviation | 1.679 | 32.46 | 33.65 | 13.57 | 1.346 | 0.46 | 0.09 | 2.346 | 1.796 | 0.3469 | 0.05 | 5346.39 |
| | P value | 5.96 E-4 | 6.83 E-6 | 6.94 E-6 | 8.35 E-7 | 7.82 E-7 | 5.93 E-6 | 6.52 E-6 | 7.92 E-3 | 7.16 E-3 | 5.07 E-4 | 3.26 E-4 | 0.01 |
| | Percentage difference 1/ND – 2/ND | **16.901** | **7.621** | **8.893** | **21.320** | **113.130** | **25.413** | **98.117** | **5.237** | **5.187** | **59.807** | **96.193** | **23.766** |
| | Difference P value | **7.62 E-6** | **4.91 E-8** | **2.97 E-8** | **7.42 E-9** | **5.39 E-9** | **6.24 E-8** | **9.43 E-8** | **4.85 E-5** | **8.17 E-5** | **6.82 E-6** | **4.71 E-6** | **5.62 E-4** |

Table 6 shows that the operator aware bandwidth management algorithm has better performance as compared to the optimized rates algorithm in the case of

disturbance presence. The conducted results show that the operator aware algorithm requires 16.901% less execution time and 23.766% less used bandwidth for the task execution. Besides, table 6 shows the superiority of the operator aware algorithm in terms of the covered distance by both robots in addition to the average distance to obstacle (DTO) measured by both robots; as well as the exit time and exit distance.

### 5.5.3 *Experimental Results Summary of two-level controller*

Table 7 presents the experimental results summary of the designed two-level controller.

*Table 7 Experimental Results for the designed two-level controller*

| | | Duration (sec) | DistR1 (mm) | DistR2 (mm) | Exit DistR1 (mm) | Exit DistR2 (mm) | Exit TimeR1 | Exit TimeR2 | Average DTO1 (mm) | Average DTO2 (mm) | Average HorError (mm) | Average VerError (mm) | Average Bw (bps) |
|---|---|---|---|---|---|---|---|---|---|---|---|---|---|
| 2/D | Average | 24.168 | 1167 | 1157 | 42.59 | 4.873 | 1.24 | 0.24 | 178.269 | 172.364 | 5.016 | 0.418 | 736942 |
| | Standard Deviation | 1.756 | 34.59 | 38.67 | 19.57 | 3.672 | 0.48 | 0.124 | 2.876 | 1.879 | 0.3896 | 0.06 | 5462.2 |
| | P value | 6.94 E-4 | 8.26 E-6 | 6.94 E-6 | 9.74 E-7 | 8.25 E-7 | 6.79 E-6 | 7.68 E-6 | 7.96 E-3 | 7.43 E-3 | 5.28 E-4 | 4.63 E-4 | 0.0118 |
| 2/ ND | Average | 22.436 | 1136 | 1096 | 37.42 | 4.35 | 1.137 | 0.23 | 167.346 | 163.649 | 4.837 | 0.409 | 729645 |
| | Standard Deviation | 1.679 | 32.46 | 33.65 | 13.57 | 1.346 | 0.46 | 0.09 | 2.346 | 1.796 | 0.3469 | 0.05 | 5346.39 |
| | P value | 5.96 E-4 | 6.83 E-6 | 6.94 E-6 | 8.35 E-7 | 7.82 E-7 | 5.93 E-6 | 6.52 E-6 | 7.92 E-3 | 7.16 E-3 | 5.07 E-4 | 3.26 E-4 | 0.01 |

Table 7 shows that the operator aware bandwidth management algorithm offers the operator similar experience in both scenarios: disturbance presence and disturbance absence. The conducted results show that the operator aware algorithm has similar performance measures in both scenarios.

### 5.5.4 *NASA Disturbance Presence Results*

The qualitative results of the NASA-TLX survey results for the disturbance presence scenario and the disturbance absence scenario are shown in Table 8 and 9 respectively. Lower workload values designate that the conducted teleoperation task has low physical and mental demands, and its pace was not rushed or hurried. Likewise, lower performance value shows that the participants were pleased with their results while achieving the collaborative teleoperation task objectives. Similarly, low effort index designates that the participants has a little workload to achieve their performance level. Lastly, low frustration index shows that participants were not stressed or discouraged within the task.

*Table 8 NASA form disturbance presence scenario results*

| | | Mental Demand | Physical Demand | Temporal Demand | Performance | Effort | Frustration |
|---|---|---|---|---|---|---|---|
| **1/D** | Average | 8.33 | 5.60 | 7.73 | 6.67 | 6.77 | 6.63 |
| | P value | 2.504E-06 | 1.840E-06 | 2.397E-09 | 4.038E-05 | 8.406E-11 | 2.609E-10 |
| **2/D** | Average | 7.6 | 4.77 | 7.1 | 5.27 | 5.4 | 5.3 |
| | P value | 3.399E-10 | 5.545E-07 | 1.221E-12 | 0.0076 | 1.713E-09 | 0.000282 |
| | Percentage difference 1/D – 2/D | **9.21** | **16.08** | **8.54** | **23.46** | **22.47** | **22.35** |
| | Difference P value | **1.89E-104** | **3.883E-35** | **3.335E-84** | **4.52E-29** | **5.866E-33** | **3.112E-29** |

Table 8 shows that the operator aware bandwidth management algorithm according to the operators' feedback has better performance than the optimized rates algorithm in the case of disturbance presence in all the 6 monitored aspects. The performance is 23.46% better knowing that it requires 22.47% less effort and causes 22.35% less frustration along with major lower demands for the conducted teleoperation task.

### 5.5.5 *NASA Disturbance Absence Results*

Table 9 presents the NASA-TLX survey results summary for the disturbance absence scenario.

*Table 9 NASA form disturbance absence scenario results*

| | | Mental Demand | Physical Demand | Temporal Demand | Performance | Effort | Frustration |
|---|---|---|---|---|---|---|---|
| **1/ND** | Average | 4.7 | 3.67 | 7.5 | 4.73 | 4.43 | 3.83 |
| | P value | 0.000803 | 0.003863 | 2.425E-15 | 1.285E-08 | 4.554E-06 | 0.000131 |
| **2/ND** | Average | 4.17 | 3.47 | 6.50 | 4.20 | 4.63 | 3.63 |
| | P value | 0.00428 | 0.0141 | 3.565E-19 | 7.533E-06 | 7.597E-09 | 3.344E-05 |
| | Percentage difference 1/ND – 2/ND | **12.030** | **5.607** | **14.286** | **11.940** | **-4.412** | **5.357** |
| | Difference P value | **7.862E-53** | **4.720E-63** | **3.377E-150** | **6.226E-140** | **0** | **0** |

Table 9 shows that, for the disturbance free case, the operator aware bandwidth management algorithm performs generally better than the optimized rates algorithm. The performance is 11.94% better with 5.357% less frustration but 4.412% more effort. This result is due to the added complexity of the operator-aware algorithm (which is the two-level controller) which requires more effort from the user as compared to the optimized rates algorithm. However, the operator aware algorithm requires less mental, physical, and temporal demands compared to the optimized rates algorithm for the conducted teleoperation task.

# CHAPTER 6

# CONCLUSION AND FUTURE WORK

This thesis presents operator-based dynamic bandwidth management for teleoperation. The most relevant work in the domains of collaborative robots, teleoperation, bandwidth management and human machine interface was presented first. This thesis integrates the PF into the bandwidth scheme through a two-level controller which dynamically updates the corresponding real-time distribution of the available bandwidth among the R2U, R2R and U2R communication channels in a way to optimize performance, upon receiving a new set of real-time observations. These observations reflect 1) changes in the *PF* through the changes in the level of disturbance encountered by the operator, 2) changes in *QoC* of the executed task, along with 3) the occurrence of *IEs* in the swarm's environment. Thus, this ensures the effective accomplishment of the collaborative task with lower bandwidth consumption and better performance.

The designed closed-loop two-level controller is implemented in a way to mimic the human mind set and cope with the need of adaptively updating the bandwidth distribution to optimize the user experience and hence the task performance. Where level 1 is an event-based fuzzy logic controller triggered by the performance measures sent by the robot and results in the appropriate set of constraints for the M matrix accordingly, this real-time set of constraints is then feed to the level 2 time-based triggered Lagrange optimization algorithm which will determine accordingly the updated set of R2U, R2R and U2R communication channels' rates introducing the

appropriate bandwidth distribution. This way the implemented two-level controller will ensure that the M matrix will dynamically adapt with the IEs, QoC and PF to ensure the optimum distribution of the available bandwidth in real-time.

This detailed problem formulation is then followed by the MATLAB implementation of the designed two-level controller, which is then tested and compared to the previously implemented dynamic bandwidth management scheme designed by Mansour [1]. This preliminary testing is then followed by a detailed MATLAB simulation integrating the implemented two-level controller into a specific collaborative task where the operator is asked to navigate 2 humanoid robots through a predefined path while avoiding the obstacles throughout this path. The simulation considers both implemented two-level controller and implemented dynamic bandwidth management scheme designed by Mansour [1] and compares both algorithms in the case of disturbance presence and disturbance absence in a way to integrate the PF as a major factor for the bandwidth distribution scheme.

This simulation is followed by another simulation using WEBOTS to scale up the task conditions along with the corresponding number of robots, this simulation is used to show the efficiency and the applicability of the implemented two-level controller in more complicated tasks. The simulation is followed then by the experimentation part, which implements the designed two-level controller in a daily life application. The experimental part is done through a MATLAB implementation of the designed two-level controller, where the proposed algorithm is evaluated against the dynamic bandwidth management algorithm presented by Mansour [1, 2].

The experiment is designed to be used with a force feedback joystick (Microsoft SideWinder Force Feedback 2), which is a standard gaming joystick, to navigate 2 humanoid robots through a delimited path to reach a predetermined destination while avoiding obstacles and preserving a formation (60 cm that separates the 2 robots in the horizontal direction while being aligned along the vertical direction). During the experiment, participants are required to control the 2 humanoid robots through a predefined track while avoiding the track obstacles; this task will be done over traditional bandwidth method and the novel 2 level control method for the bandwidth division with differentiating 2 cases for each method, one with disturbance presence and one without disturbance. Furthermore, the disturbance is done through Delayed Digital Recall (n-back) task, which is a calibration method developed by the MIT AgeLab that systematically increases the cognitive demand placed on an individual. This task was used in a series of driver workload and distraction studies [36].

Both the simulation and the experimental parts show the superiority of the designed 2 level controller over the traditional dynamic bandwidth management algorithm in terms of task performance and bandwidth distribution; where the collaborative task is accomplished with higher levels of cooperation.

As future work, it is necessary to integrate a social/behavioral part to be cascaded to the designed 2 level controller in a way to have a systematic way to measure and determine the exact level of disturbance encountered by the operator. This tasks includes specifying the appropriate factors to consider and monitor accordingly to measure the encountered level of disturbance and hence establish a well-defined methodology to specify the accurate value for the PF variable in real time. This development requires studying the various social/behavioral variables that will change

upon the teleoperation task and accordingly specify which variables are relevant to be integrated into the bandwidth management scheme through specifying the appropriate sensors and data acquisition methods.

Additionally, it is worth accounting for the case of variable total bandwidth available for the collaborative teleoperation task. In other words, it will add to the algorithm efficiency and robustness having into consideration the fact of variable available bandwidth as a major factor to account for upon the process of specifying the optimal allocation of the communication rates.

Besides, it is required to consider the presented scaling up simulation to design more complex experimental tasks with swarms of 3 or more heterogeneous robots to elaborately test the designed 2 level dynamic bandwidth management controller. Hence it is advised to test the presented algorithm to execute a variety of more complex collaborative scenarios to assure the efficiency of the designed operator-aware bandwidth management method.

# REFERENCES

[1] Mansour C., Elhariri M., Elhajj I.H., Shammas E., Asmar D. Dynamic Optimized Bandwidth Management for Teleoperation of Collaborative Robots. Book Article "Recent Advances in Robotic Systems" book edited by Guanghui Wang, ISBN 978-953-51-2571-6, Print ISBN 978-953-51-2570-9, Published: September 28, 2016 CC BY 3.0 license.

[2] Mansour C., Elhajj I.H., Shammas E., Asmar D. Event-based dynamic bandwidth management for teleoperation. In: 2011 IEEE international conference on robotics and biomimetics (ROBIO), 7‑11 Dec.2011; Karon Beach, Phuket. IEEE; 2011. p. 229‑233. doi: 10.1109/ROBIO.2011.6181290

[3] Elmasry A., and Liermann M. PASSIVE PNEUMATIC TELEOPERATION SYSTEM. Proceedings of the ASME/BATH 2013 Symposium on Fluid Power & Motion Control FPMC2013 October 6-9, 2013, Sarasota, Florida, USA FPMC2013-4464.

[4] Lee D., Spong M.W. Semi autonomous teleoperation of multiple cooperative robots for human robot exploration. In: Proceedings of the AAAI 2006 Spring Symposium; Palo alto, California, USA, 2006.

[5] Schenker P.S., Huntsberger T.L., Pirjanian P., Baumgartner E.T., Tunstel E. Planetary rover developments supporting mars exploration, sample return and future humanrobotic colonization. Autonomous Robots. 2003; 14(2‑3):103‑126. doi:10.1023/A: 1022271301244

[6] Hwanga G., Szemesb P.T., Andoc N., Hashimotod H. Development of a single-master multi-slave tele-micromanipulation system. Advanced Robotics. 2007; 21(3–4):329–349. doi:10.1163/156855307780132054

[7] Liermann M., Baayoun M.A., and Daher N. ADAPTIVE CONTROLLER DESIGN OF MRI COMPATIBLE PNEUMATIC TELE-OPERATION SYSTEM. Proceedings of the ASME/BATH 2015 Symposium on Fluid Power & Motion Control FPMC2015 October 12-14, 2015, Chicago, Illinois, United States.

[8] Thomson J.M., Ottensmeyer M.P., Sheridan T.B. Human factors in telesurgery: effects of time delay and asynchrony in video and control feedback with local manipulative assistance. Telemedicine Journal. 1999;5(2):129–137. doi:10.1089/107830299312096.

[9] Li H., Tadano K., Kawashima K., 2015, "Experimental Validation of Stability and Performance for Position-Error-Based Tele-surgery," International Conference on Advanced Intelligent Mechatronics (AIM), IEEE, pp. 848- 853.

[10] Ehajj I., Xi N., Fung W.K., Liu Y.H., Hasegawa Y., Fukuda T. Supermedia-enhanced internet-based telerobotics. Proceedings of the IEEE. 2003; 91(3):396–421. doi:10.1109/ JPROC.2003.809203

[11] Wai- keung Fung et al., "Task driven dynamic QoS based bandwidth allocation for realtime teleoperation via the Internet," Intelligent Robots and Systems, 2003. (IROS 2003). Proceedings. 2003 IEEE/RSJ International Conference on, Las Vegas, Nevada, USA 2003, pp. 1094–1099 vol.2. doi: 10.1109/IROS.2003.1248790

[12] P. Berthet-Rayne, M. Power, H. King and G. Z. Yang, "Hubot: A three state Human-Robot collaborative framework for bimanual surgical tasks based on learned models," 2016 IEEE International Conference on Robotics and Automation (ICRA), Stockholm, 2016, pp. 715-722. doi:10.1109/ICRA.2016.7487198

[13] M. Power, H. Rafii-Tari, C. Bergeles, V. Vitiello and Guang-Zhong Yang, "A cooperative control framework for haptic guidance of bimanual surgical tasks based on Learning from Demonstration," 2015 IEEE International Conference on Robotics and Automation (ICRA), Seattle, WA, 2015, pp.5330-5337. doi:10.1109/ICRA.2015.7139943

[14] Mourikis A.I., Roumeliotis S.I. Optimal sensor scheduling for resource-constrained localization of mobile robot formations. IEEE Transactions on Robotics. 2006; 22(5):917–931. doi:10.1109/TRO.2006.878947

[15] Sugiyama H., Tsujioka T., Murata M. Integrated operations of multi-robot rescue system with Ad Hoc networking. In: 1st International conference on wireless communication, vehicular technology, information theory and aerospace & electronic systems technology, 2009. Wireless VITAE 2009; 17–20 May 2009; Aalborg. IEEE; 2009. p. 535– 539. doi:10.1109/WIRELESSVITAE.2009.5172502

[16] Bhuvanagiri S., Krishna M.K., Achar S. Coordination in ambiguity: coordinated active localization for multiple robots. In: AAMAS (Demo Paper); Estoril, Portugal, 2008; 1707– 1708. doi: 10.1016/j.robot.2009.09.006

[17] Andre T., Bettstetter T. Collaboration in multi-robot exploration: to meet or not to meet? Journal of Intelligent & Robotic Systems. 2015; 1–13. doi:10.1007/s10846-015-0277-0

[18] M. Kudelski, L. M. Gambardella and G. A. Di Caro, "A mobility-controlled link quality learning protocol for multi-robot coordination tasks," 2014 IEEE International Conference on Robotics and Automation (ICRA), Hong Kong, 2014, pp. 5024-5031. doi:10.1109/ICRA.2014.6907595

[19] M. Mostefa. L. Kaddour El Boudadi. J. Vareille. "Safe and efficient mobile robot teleoperation via a network with communication delay" Springer-Verlag France 2017. pp. 1-6. doi:10.1007/s12008-017-0370-7

[20] Wang X., Chen M., Huang H.M., Subramonian V., Lu C., Gill C.D. Control-based adaptive middleware for real-time image transmission over bandwidth-constrained networks. IEEE Transactions on Parallel and Distributed Systems. 2008;19(6):779–793. doi:10.1109/TPDS.2008.41

[21] Phillips-Grafflin C., Suay H.B., Mainprice J., Alunni N., Lofaro D., Berenson D., Chernova S., Lindeman R.W., Oh P. From autonomy to cooperative traded control of humanoid manipulation tasks with unreliable communication. Journal of Intelligent & Robotic Systems. 2015; 1–21. doi:10.1007/s10846-015-0256-5

[22] Wai-keung Fung, Ning Xi, Wang-tai Lo and Yun-hui Liu, "Improving efficiency of Internet based teleoperation using network QoS," Proceedings 2002 IEEE International Conference on Robotics and Automation (Cat. No.02CH37292), Washington, DC, 2002, pp. 2707-2712. doi:10.1109/ROBOT.2002.1013641

[23] L. Roche and L. Saint-Bauzel, "Implementation of haptic communication in comanipulative tasks: A statistical state machine model," 2016 IEEE/RSJ International Conference on Intelligent Robots and Systems (IROS), Daejeon, 2016, pp. 2670-2675. doi:10.1109/IROS.2016.7759415

[24] P. Bremner and U. Leonards, "Efficiency of speech and iconic gesture integration for robotic and human communicators - a direct comparison," 2015 IEEE International Conference on Robotics and Automation (ICRA), Seattle, WA, 2015, pp. 1999-2006. doi:10.1109/ICRA.2015.7139460

[25] Jingting Sun, Hui Li, Jinchen An, Kai Pan and Jun Lu, "An efficient transmission scheme for data aggregation in wireless sensor networks," 2016 IEEE Symposium on Computers and Communication (ISCC), Messina, 2016, pp. 64-68. doi:10.1109/ISCC.2016.7543715

[26] I. H. Brahmi, S. Djahel, D. Magoni and J. Murphy, "An efficient partial data aggregation scheme in WSNs," 2014 IFIP Wireless Days (WD), Rio de Janeiro, 2014, pp. 1-3. doi: 10.1109/WD.2014.7020845

[27] A. Manzi, L. Fiorini, R. Limosani, P. Sincak, P. Dario and F. Cavallo, "Use Case Evaluation of a Cloud Robotics Teleoperation System (Short Paper)," 2016 5th IEEE International Conference on Cloud Networking (Cloudnet), Pisa, 2016, pp. 208-211. doi:10.1109/CloudNet.2016.49

[28] S. Merlin, N. Vaidya and M. Zorzi, "Resource Allocation in Multi-Radio Multi-Channel Multi-Hop Wireless Networks," IEEE INFOCOM 2008 - The 27th Conference on Computer Communications, Phoenix, AZ, 2008, pp. doi:10.1109/INFOCOM.2008.110

[29] Chaskar H.M., Madhow U. Fair scheduling with tunable latency: a round-robin approach. IEEE/ACM Transactions on Networking. 2003; 11(4):592‑601. doi:10.1109/TNET.2003.815290

[30] Tipsuwan Y., Kamonsantiroj S., Srisabye J., Chongstitvattana P. An auction-based dynamic bandwidth allocation with sensitivity in a wireless networked control system. Computers & Industrial Engineering. 2008; 47:114–124. doi: 10.1016/j.cie.2008.08.018

[31] L. G. Torres et al., "A motion planning approach to automatic obstacle avoidance during concentric tube robot teleoperation," 2015 IEEE International Conference on Robotics and Automation (ICRA), Seattle, WA,2015, pp.2361-2367. doi:10.1109/ICRA.2015.7139513

[32] M. Panzirsch, R. Balachandran and J. Artigas, "Cartesian task allocation for cooperative, multilateral teleoperation under time delay," 2015 IEEE International Conference on Robotics and Automation (ICRA), Seattle, WA,2015, pp.312-317. doi:10.1109/ICRA.2015.7139017

[33] P. Lehner, A. Sieverling and O. Brock, "Incremental, sensor-based motion generation for mobile manipulators in unknown, dynamic environments," 2015 IEEE International Conference on Robotics and Automation (ICRA), Seattle, WA, 2015, pp. 4761-4767.
doi:10.1109/ICRA.2015.7139861

[34] I. Nisky, Y. Che, Z. F. Quek, M. Weber, M. H. Hsieh and A. M. Okamura, "Teleoperated versus open needle driving: Kinematic analysis of experienced surgeons and novice users," 2015 IEEE International Conference on Robotics and Automation (ICRA), Seattle, WA, 2015, pp. 5371-5377. doi:10.1109/ICRA.2015.7139949

[35] Julio R.E., Bastos G.S., Dynamic bandwidth management library for multi-robot systems. In: 2015 IEEE/RSJ International Conference on Intelligent Robots and Systems (IROS), Hamburg. 2015; 2585–2590. doi:10.1109/IROS.2015.7353729

[36] Rana Tarabay, Maya Abou-Zeid, Assessing the effects of auditory-vocal distraction on driving performance and physiological measures using a driving simulator, Transportation Research Part F: Traffic Psychology and Behaviour, Volume 58, 2018, Pages 351-364, ISSN 1369-8478, https://doi.org/10.1016/j.trf.2018.06.026.

[37] I.R. Nourbakhsh, K. Sycara, M. Koes, M. Yong, M. Lewis, and S. Burion, "Human robot teaming for search and rescue". Pervasive Computing, IEEE, pp.72–79, March 2005.
[38] Xinda Song, Xiangwei Hao, Huaping Liu, Kezhong He, Meng Gao, "Teleoperation system for multiple mobile robots". Control and Decision Conference (CCDC), 2011 Chinese, pp.555-560, 23-25 May 2011.

[39] Palafox O.M., Spong M.W., "Bilateral teleoperation of a formation of nonholonomic mobile robots under constant time delay". Intelligent Robots and Systems, 2009. IROS 2009. IEEE/RSJ International Conference on, pp.2821-2826, 10-15 Oct. 2009.

[40] MacArthur, D.K., Crane, C.D, " Unmanned Ground Vehicle State Estimation using an Unmanned Air Vehicle". Computational Intelligence in Robotics and Automation, 2007, International Symposium on, pp.473-478, 20-23 June 2007.

[41] Dapeng Jiang, Yongjie Pang, Zaibai Qin, " Coordinated control of multiple autonomous underwater vehicle system". Intelligent Control and Automation (WCICA), 2010 8th World Congress on, pp.4901-4906, 7-9 July 2010.

[42] Hu, Y., Wang, L., Liang, J., Wang, T., "Cooperative box-pushing with multiple autonomous robotic fish in underwater environment". Control Theory & Applications, IET, vol.5, no.17, pp.2015-2022, Nov 2011.

[43] Maithripala, D.H.A., Jayasuriya, S., "Feasibility considerations in formation control: Phantom track generation through multi-UAV collaboration". Decision and Control, 2008. CDC 2008. 47th IEEE Conference on, pp.3959-3964, 9-11 Dec. 2008.

[44] T. Langner, D. Seifert, B. Fischer, D. Goehring, T. Ganjineh and R. Rojas, “Traffic awareness driver assistance based on stereovision, eye-tracking, and head-up display”; 2016 IEEE International Conference on Robotics and Automation (ICRA), Stockholm, 2016, pp. 3167-3173. doi:10.1109/ICRA.2016.7487485.

[45] Anbin Xiong, Xingang Zhao, Jianda Han, G. Liu and Qichuan Ding, "An user-independent gesture recognition method based on sEMG decomposition”; 2015 IEEE/RSJ International Conference on Intelligent Robots and Systems (IROS), Hamburg, 2015, pp. 4185-4190. doi:10.1109/IRO S.2015.7353969.

[46] K. Nakadai, T. Mizumoto and K. Nakamura, "Robot-Audition-based Human-Machine Interface for a Car"; 2015 IEEE/RSJ International Conference on Intelligent Robots and Systems (IROS), Hamburg, 2015, pp. 6129-6136. doi:10.1109/IROS.2015.7354250

# APPENDIX

## *NASA Task Load Index*

*Hart and Staveland's NASA Task Load Index (TLX) method assesses work load on five 7-point scales. Increments of high, medium and low estimates for each point result in 21 gradations on the scales.*

| Name | Task | Date |
|---|---|---|
| | | |

Mental Demand — How mentally demanding was the task?

Very Low — Very High

Physical Demand — How physically demanding was the task?

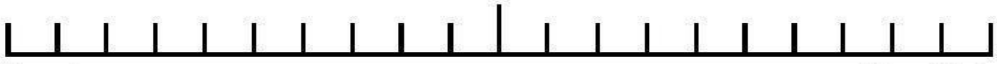

Very Low — Very High

Temporal Demand — How hurried or rushed was the pace of the task?

Very Low — Very High

Performance — How successful were you in accomplishing what you were asked to do?

Perfect — Failure

Effort — How hard did you have to work to accomplish your level of performance?

Very Low — Very High

Frustration — How insecure, discouraged, irritated, stressed, and annoyed wereyou?

Very Low — Very High